

NEUTRAL PSEUDOSCALAR AND VECTOR MESON MASSES  
UNDER STRONG MAGNETIC FIELDS IN AN EXTENDED NJL  
MODEL: MIXING EFFECTS

J.P. Carlomagno<sup>a,b</sup>, D. Gómez Dumm<sup>a,b</sup>, S. Noguera<sup>c</sup> and N.N. Scoccola<sup>b,c,d</sup>

<sup>a</sup> *IFLP, CONICET – Departamento de Física,  
Facultad de Ciencias Exactas, Universidad Nacional de La Plata,  
C.C. 67, (1900) La Plata, Argentina*

<sup>b</sup> *CONICET, Rivadavia 1917, (1033) Buenos Aires, Argentina*

<sup>c</sup> *Departamento de Física Teórica and IFIC,  
Centro Mixto Universidad de Valencia-CSIC,  
E-46100 Burjassot (Valencia), Spain and*

<sup>d</sup> *Physics Department, Comisión Nacional de Energía Atómica,  
Av. Libertador 8250, (1429) Buenos Aires, Argentina*

(Dated: June 1, 2022)

## Abstract

Mixing effects on the mass spectrum of light neutral pseudoscalar and vector mesons in the presence of an external uniform magnetic field  $\vec{B}$  are studied in the framework of a two-flavor NJL-like model. The model includes isoscalar and isovector couplings both in the scalar-pseudoscalar and vector sectors, and also incorporates flavor mixing through a 't Hooft-like term. Numerical results for the  $B$  dependence of meson masses are compared with present lattice QCD results. In particular, it is shown that the mixing between pseudoscalar and vector meson states leads to a significant reduction of the mass of the lightest state. The role of chiral symmetry and the effect of the alignment of quark magnetic moments in the presence of the magnetic field are discussed.

## I. INTRODUCTION

It is well known that the presence of a large background magnetic field  $\vec{B}$  has a significant impact on the physics of strongly interacting particles, leading to important effects on both hadron properties and QCD phase transition features [1–3]. By a “large” field it is understood here that the order of magnitude of  $B$  competes with the QCD confining scale  $\Lambda_{\text{QCD}}$  squared, i.e.  $|eB| \gtrsim \Lambda_{\text{QCD}}^2$ ,  $|B| \gtrsim 10^{19}$  G. Such huge magnetic fields can be achieved in matter at extreme conditions, e.g. at the occurrence of the electroweak phase transition in the early Universe [4, 5] or in the deep interior of compact stellar objects like magnetars [6, 7]. Moreover, it has been pointed out that values of  $|eB|$  ranging from  $m_\pi^2$  to  $15 m_\pi^2$  ( $|B| \sim 0.3$  to  $5 \times 10^{19}$  G) can be reached in noncentral collisions of relativistic heavy ions at RHIC and LHC experiments [8, 9]. Though these large background fields are short lived, they should be strong enough to affect the hadronization process, offering the amazing possibility of recreating a highly magnetized QCD medium in the lab.

From the theoretical point of view, the study of strong interactions in the presence of a large magnetic field includes several interesting phenomena, such as the chiral magnetic effect [10–12], which entails the generation of an electric current induced by chirality imbalance, and the so-called magnetic catalysis [13, 14] and inverse magnetic catalysis [15, 16], which refer to the effect of the magnetic field on the size of chiral quark-antiquark condensates and on the restoration of chiral symmetry. Yet another interesting issue is the possible existence of a phase transition of the cold vacuum into an electromagnetic superconducting state. For a sufficiently large external magnetic field, this transition would be induced by

the emergence of quark-antiquark vector condensates that carry the quantum numbers of electrically charged  $\rho$  mesons [17, 18]. The presence of such a superconducting (anisotropic and inhomogeneous) QCD vacuum state has been discussed in the past few years and still remains as an open problem [19–22].

It is clear that the study of the properties of light hadrons, in particular  $\pi$  and  $\rho$  mesons, comes up as a crucial task towards the understanding of the above mentioned phenomena. This represents a nontrivial problem, since first-principle theoretical calculations require to deal in general with QCD in a low energy nonperturbative regime. Therefore, the corresponding theoretical analyses have been carried out using a variety of effective models for strong interactions. The effect of intense external magnetic fields on  $\pi$  meson properties has been studied e.g. in the framework of Nambu-Jona-Lasinio (NJL)-like models [23–38], quark-meson models [39, 40], chiral perturbation theory (ChPT) [41–43], path integral Hamiltonians [44, 45], effective chiral confinement Lagrangians [46, 47] and QCD sum rules [48]. In addition, several results for the  $\pi$  meson spectrum in the presence of background magnetic fields have been obtained from lattice QCD (LQCD) calculations [15, 49–53]. Regarding the  $\rho$  meson sector, studies of magnetized  $\rho$  meson masses in the framework of effective models and LQCD can be found in Refs. [18, 28, 31, 36, 45, 54–57] and Refs. [49, 50, 52, 58, 59], respectively.

In this work we study the mass spectrum of light neutral pseudoscalar and vector mesons in the presence of an external uniform magnetic field  $\vec{B}$ , considering a two-flavor NJL-like model [60–62]. In general, in this type of model the calculations involving quark loops for nonzero  $B$  include the so-called Schwinger phases [63], which are responsible for the breakdown of translational invariance of quark propagators. However, in the particular case of neutral mesons these phases cancel out, and one is free to take the usual momentum basis to diagonalize the corresponding polarization functions [23–27]. One also has to care about the regularization procedure, since the presence of the external field can lead to spurious results, such as unphysical oscillations of various observables [64, 65]. We consider here a magnetic field independent regularization (MFIR) method [25, 26, 32, 66], which has been shown to be free from these effects and reduces the dependence of the results on model parameters. In addition, in our work we consider two mixing effects that have been mostly neglected in previous analyses. The first one is flavor mixing in the spin zero sector; while we restrict to a two-flavor model (keeping a reduced number of free parameters, and

assuming that strangeness does not play an essential role), we consider quark-antiquark interactions both in  $I = 1$  and  $I = 0$  scalar and pseudoscalar channels, introducing a 't Hooft-like effective interaction [67]. The second one is the mixing between pseudoscalar and vector mesons, which arises naturally in the context of the NJL model. These mixing contributions are usually forbidden by isospin and angular momentum conservation, but they arise (and may become important) in the presence of the external magnetic field. In fact, our analysis shows that  $\pi^0$  -  $\eta$  -  $\rho^0$  -  $\omega$  mixing has a substantial effect on the  $B$  dependence of the lowest mass state. As a additional ingredient, we consider the case of  $B$ -dependent effective coupling constants; this possibility —inspired by the magnetic screening of the strong coupling constant occurring for large  $B$  [68]— has been previously explored in effective models [37, 69–72] in order to reproduce the inverse magnetic catalysis effect observed at finite temperature in LQCD calculations.

In the case of the neutral vector mesons, we consider both states with quantum numbers  $S_z = 0$  and  $S_z = \pm 1$ , where  $S_z$  is the spin projection in the direction of the magnetic field (it is worth noticing that only  $S_z = 0$  states can mix with pseudoscalar states). Most LQCD results and effective model calculations agree in the finding that the masses of  $S_z = \pm 1$  states get monotonically enhanced with the magnetic field, while results for  $S_z = 0$  mesons are still not conclusive [31, 45, 49, 50, 52, 57, 58]. In our framework, which lacks a description of confinement, for large magnetic fields the masses of some of the  $S_z = 0$  states are found to grow beyond the  $q\bar{q}$  pair production threshold; therefore our results in this region should be taken just as qualitative ones.

The paper is organized as follows. In Sec. II we introduce the theoretical formalism used to obtain neutral pseudoscalar and vector meson masses. Then, in Sec. III we present and discuss our numerical results, while in Sec. IV we provide a summary of our work, together with our main conclusions. We also include Appendixes A, B and C to provide some technical details of our calculations.

## II. THEORETICAL FORMALISM

### A. Effective Lagrangian and mean field properties

Let us start by considering the Euclidean Lagrangian density for an extended NJL two-flavor model in the presence of an electromagnetic field. We have

$$\begin{aligned} \mathcal{L} = & \bar{\psi}(x) (-i\not{D} + m_c) \psi(x) - g_s \sum_{a=0}^3 \left[ (\bar{\psi}(x) \tau_a \psi(x))^2 + (\bar{\psi}(x) i\gamma_5 \tau_a \psi(x))^2 \right] \\ & - g_{v_3} (\bar{\psi}(x) \gamma_\mu \vec{\tau} \psi(x))^2 - g_{v_0} (\bar{\psi}(x) \gamma_\mu \psi(x))^2 + 2g_d (d_+ + d_-) , \end{aligned} \quad (1)$$

where  $\psi = (u \ d)^T$ ,  $\tau_a = (\mathbb{1}, \vec{\tau})$ ,  $\vec{\tau}$  being the usual Pauli-matrix vector, and  $m_c$  is the current quark mass, which is assumed to be equal for  $u$  and  $d$  quarks. The model includes isoscalar and isovector vector couplings, and also a 't Hooft-like flavor-mixing term where we have defined  $d_\pm = \det[\bar{\psi}(x)(1 \pm \gamma_5)\psi(x)]$ . The interaction between the fermions and the electromagnetic field  $\mathcal{A}_\mu$  is driven by the covariant derivative

$$D_\mu = \partial_\mu - i\hat{Q}\mathcal{A}_\mu , \quad (2)$$

where  $\hat{Q} = \text{diag}(Q_u, Q_d)$ , with  $Q_u = 2e/3$  and  $Q_d = -e/3$ ,  $e$  being the proton electric charge. We consider the particular case in which one has a homogenous stationary magnetic field  $\vec{B}$  orientated along the 3, or  $z$ , axis. Then, choosing the Landau gauge, we have  $\mathcal{A}_\mu = B x_1 \delta_{\mu 2}$ .

Since we are interested in studying meson properties, it is convenient to bosonize the fermionic theory, introducing scalar, pseudoscalar and vector fields  $\sigma_a(x)$ ,  $\pi_a(x)$  and  $\rho_{a\mu}(x)$ , with  $a = 0, 1, 2, 3$ , and integrating out the fermion fields. The bosonized Euclidean action can be written as

$$\begin{aligned} S_{\text{bos}} = & -\ln \det \mathcal{D} + \frac{1}{4g} \int d^4x \left[ \sigma_0(x) \sigma_0(x) + \vec{\pi}(x) \cdot \vec{\pi}(x) \right] \\ & + \frac{1}{4g(1-2\alpha)} \int d^4x \left[ \vec{\sigma}(x) \cdot \vec{\sigma}(x) + \pi_0(x) \pi_0(x) \right] \\ & + \frac{1}{4g_{v_3}} \int d^4x \vec{\rho}_\mu(x) \cdot \vec{\rho}_\mu(x) + \frac{1}{4g_{v_0}} \int d^4x \rho_{0\mu}(x) \rho_{0\mu}(x) , \end{aligned} \quad (3)$$

with

$$\mathcal{D}_{x,x'} = \delta^{(4)}(x - x') \left[ -i\not{D} + m_0 + \tau_a (\sigma_a(x) + i\gamma_5 \pi_a(x) + \gamma_\mu \rho_{a\mu}(x)) \right] , \quad (4)$$

where a direct product to an identity matrix in color space is understood. Note that for convenience we have introduced the combinations

$$g = g_s + g_d , \quad \alpha = g_d / (g_s + g_d) , \quad (5)$$

so that the flavor mixing in the scalar-pseudoscalar sector is regulated by the constant  $\alpha$ . For  $\alpha = 0$  quark flavors  $u$  and  $d$  get decoupled, while for  $\alpha = 0.5$  one has maximum flavor mixing, as in the case of the standard version of the NJL model.

We proceed by expanding the bosonized action in powers of the fluctuations of the bosonic fields around the corresponding mean field (MF) values. We assume that the fields  $\sigma_a(x)$  have nontrivial translational invariant MF values given by  $\tau_a \bar{\sigma}_a = \text{diag}(\bar{\sigma}_u, \bar{\sigma}_d)$ , while vacuum expectation values of other bosonic fields are zero; thus, we write

$$\mathcal{D}_{x,x'} = \mathcal{D}_{x,x'}^{\text{MF}} + \delta \mathcal{D}_{x,x'} . \quad (6)$$

The MF piece is diagonal in flavor space. One has

$$\mathcal{D}_{x,x'}^{\text{MF}} = \text{diag}(\mathcal{D}_{x,x'}^{\text{MF},u}, \mathcal{D}_{x,x'}^{\text{MF},d}) , \quad (7)$$

with

$$\mathcal{D}_{x,x'}^{\text{MF},f} = \delta^{(4)}(x - x') (-i\not{\partial} - Q_f B x_1 \gamma_2 + M_f) , \quad (8)$$

where  $M_f = m_c + \bar{\sigma}_f$  is the quark effective mass for each flavor  $f$ .

The MF action per unit volume is given by

$$\frac{S_{\text{bos}}^{\text{MF}}}{V^{(4)}} = \frac{(1 - \alpha)(\bar{\sigma}_u^2 + \bar{\sigma}_d^2) - 2\alpha \bar{\sigma}_u \bar{\sigma}_d}{8g(1 - 2\alpha)} - \frac{N_c}{V^{(4)}} \sum_{f=u,d} \int d^4x d^4x' \text{tr}_D \ln \left( \mathcal{S}_{x,x'}^{\text{MF},f} \right)^{-1} , \quad (9)$$

where  $\text{tr}_D$  stands for the trace in Dirac space, and  $\mathcal{S}_{x,x'}^{\text{MF},f} = (\mathcal{D}_{x,x'}^{\text{MF},f})^{-1}$  is the MF quark propagator in the presence of the magnetic field. As is well known, the explicit form of the propagators can be written in different ways [2, 3]. For convenience we take the form in which  $\mathcal{S}_{x,x'}^{\text{MF},f}$  is given by a product of a phase factor and a translational invariant function, namely

$$\mathcal{S}_{x,x'}^{\text{MF},f} = e^{i\Phi_f(x,x')} \int_p e^{ip(x-x')} \tilde{S}_p^f , \quad (10)$$

where  $\Phi_f(x, x') = q_f B(x_1 + x'_1)(x_2 - x'_2)/2$  is the so-called Schwinger phase. We have introduced here the shorthand notation

$$\int_p \equiv \int \frac{d^4p}{(2\pi)^4} . \quad (11)$$

Now  $\tilde{S}_p^f$  can be expressed in the Schwinger form [2, 3]

$$\begin{aligned} \tilde{S}_p^f &= \int_0^\infty d\tau \exp \left[ -\tau \left( M_f^2 + p_\parallel^2 + p_\perp^2 \frac{\tanh(\tau B_f)}{\tau B_f} - i\epsilon \right) \right] \\ &\times \left\{ (M_f - p_\parallel \cdot \gamma_\parallel) [1 + i s_f \gamma_1 \gamma_2 \tanh(\tau B_f)] - \frac{p_\perp \cdot \gamma_\perp}{\cosh^2(\tau B_f)} \right\} , \end{aligned} \quad (12)$$

where we have used the following definitions. The perpendicular and parallel gamma matrices are collected in vectors  $\gamma_\perp = (\gamma_1, \gamma_2)$  and  $\gamma_\parallel = (\gamma_3, \gamma_4)$ , and, similarly, we have defined  $p_\perp = (p_1, p_2)$  and  $p_\parallel = (p_3, p_4)$ . Note that we are working in Euclidean space, where  $\{\gamma_\mu, \gamma_\nu\} = -2\delta_{\mu\nu}$ . Other definitions in Eq. (12) are  $s_f = \text{sign}(Q_f B)$  and  $B_f = |Q_f B|$ . The limit  $\epsilon \rightarrow 0$  is implicitly understood.

The integral in Eq. (12) is divergent and has to be properly regularized. As stated in the Introduction, we use here the magnetic field independent regularization (MFIR) scheme: for a given unregularized quantity, the corresponding (divergent)  $B \rightarrow 0$  limit is subtracted and then it is added in a regularized form. Thus, the quantities can be separated into a (finite) “ $B = 0$ ” part and a “magnetic” piece. Notice that, in general, the “ $B = 0$ ” part still depends implicitly on  $B$  (e.g. through the values of the dressed quark masses  $M_f$ ), hence it should not be confused with the value of the studied quantity at vanishing external field. To deal with the divergent “ $B = 0$ ” terms we use here a 3D cutoff regularization scheme. In the case of the quark-antiquark condensates  $\phi_f \equiv \langle \bar{\psi}_f \psi_f \rangle$ ,  $f = u, d$ , we obtain

$$\phi_f^{\text{reg}} = \phi_f^{0,\text{reg}} + \phi_f^{\text{mag}} , \quad (13)$$

where

$$\phi_f^{0,\text{reg}} = -N_c M_f I_{1f} , \quad \phi_f^{\text{mag}} = -N_c M_f I_{1f}^{\text{mag}} . \quad (14)$$

The expression of  $I_{1f}$  for the 3D cutoff regularization is given by Eq. (A3) of App. A [61], while the  $B$ -dependent function  $I_{1f}^{\text{mag}}$  reads [13, 64]

$$I_{1f}^{\text{mag}} = \frac{B_f}{2\pi^2} \left[ \ln \Gamma(x_f) - \left( x_f - \frac{1}{2} \right) \ln x_f + x_f - \frac{\ln 2\pi}{2} \right] , \quad (15)$$

where  $x_f = M_f^2/(2B_f)$ . The corresponding gap equations, obtained from  $\partial S_{\text{bos}}^{\text{MF}}/\partial \bar{\sigma}_f = 0$ , can be written as

$$\begin{aligned} M_u &= m_c - 4g [(1 - \alpha) \phi_u^{\text{reg}} + \alpha \phi_d^{\text{reg}}] , \\ M_d &= m_c - 4g [(1 - \alpha) \phi_d^{\text{reg}} + \alpha \phi_u^{\text{reg}}] . \end{aligned} \quad (16)$$

As anticipated, for  $\alpha = 0$  these equations get decoupled. For  $\alpha = 0.5$  the right hand sides become identical, thus one has in that case  $M_u = M_d$ .

## B. Neutral meson system

As expected from charge conservation, it is easy to see that the contributions to the bosonic action that are quadratic in the fluctuations of charged and neutral mesons decouple from each other. In this work we concentrate on the neutral meson sector. For notational convenience we will denote isospin states by  $M = \sigma_a, \pi_a, \rho_{a\mu}$ , with  $a = 0, 3$ . Here  $\sigma_0, \pi_0$  and  $\rho_0$  correspond to the isoscalar states  $\sigma, \eta$  and  $\omega$ , while  $\sigma_3, \pi_3$  and  $\rho_3$  stand for the neutral components of the isovector triplets  $\vec{a}_0, \vec{\pi}$  and  $\vec{\rho}$ , respectively. Thus, the corresponding quadratic piece of the bosonized action can be written as

$$S_{\text{bos}}^{\text{quad, neutral}} = \frac{1}{2} \int d^4x d^4x' \sum_{M, M'} \delta M(x) \mathcal{G}_{MM'}(x, x') \delta M'(x'). \quad (17)$$

The functions  $\mathcal{G}_{MM'}(x, x')$  can be separated in two terms, namely

$$\mathcal{G}_{MM'}(x, x') = \frac{1}{2g_M} \delta_{MM'} \delta^{(4)}(x - x') + \mathcal{J}_{MM'}(x, x'), \quad (18)$$

where  $\delta_{MM'}$  is an obvious generalization of the Kronecker  $\delta$ , and the constants  $g_M$  are given by

$$g_M = \begin{cases} g & \text{for } M = \sigma_0, \pi_3 \\ g(1 - 2\alpha) & \text{for } M = \sigma_3, \pi_0 \\ g_{v_3} & \text{for } M = \rho_{3\mu} \\ g_{v_0} & \text{for } M = \rho_{0\mu} \end{cases}. \quad (19)$$

The polarization functions  $\mathcal{J}_{MM'}(x, x')$  can be separated into  $u$  and  $d$  quark pieces,

$$\mathcal{J}_{MM'}(x, x') = \mathcal{F}_{MM'}^u(x', x) + \varepsilon_M \varepsilon_{M'} \mathcal{F}_{MM'}^d(x', x). \quad (20)$$

Here  $\varepsilon_M = 1$  for the isoscalars  $M = \sigma_0, \pi_0, \rho_{0\mu}$  and  $\varepsilon_M = -1$  for  $M = \sigma_3, \pi_3, \rho_{3\mu}$ , while the functions  $\mathcal{F}_{MM'}^f(x', x)$  are found to be

$$\mathcal{F}_{MM'}^f(x', x) = N_c \text{tr}_D \left[ \mathcal{S}_{x, x'}^{\text{MF}, f} \Gamma^{M'} \mathcal{S}_{x', x}^{\text{MF}, f} \Gamma^M \right], \quad (21)$$

with

$$\Gamma^M = \begin{cases} 1 & \text{for } M = \sigma_0, \sigma_3 \\ i\gamma_5 & \text{for } M = \pi_0, \pi_3 \\ \gamma_\mu & \text{for } M = \rho_{0\mu}, \rho_{3\mu} \end{cases}. \quad (22)$$

As stated, since we are dealing with neutral mesons, the contributions of Schwinger phases associated with the quark propagators in Eq. (10) cancel out, and the polarization functions



depend only on the difference  $x - x'$ , i.e., they are translationally invariant. After a Fourier transformation, the conservation of momentum implies that the polarization functions turn out to be diagonal in the momentum basis. Thus, in this basis the neutral meson contribution to the quadratic action can be written as

$$S_{\text{bos}}^{\text{quad, neutral}} = \frac{1}{2} \sum_{M, M'} \int_q \delta M(-q) G_{MM'}(q) \delta M'(q) . \quad (23)$$

Now we have

$$G_{MM'}(q) = \frac{1}{2g_M} \delta_{MM'} + J_{MM'}(q) , \quad (24)$$

and the associated polarization functions are given by

$$J_{MM'}(q) = F_{MM'}^u(q) + \varepsilon_M \varepsilon_{M'} F_{MM'}^d(q) . \quad (25)$$

The functions  $F_{MM'}^f(q)$  read

$$F_{MM'}^f(q) = N_c \int_p \text{tr}_D \left[ \tilde{S}_{p+}^f \Gamma^{M'} \tilde{S}_{p-}^f \Gamma^M \right] , \quad (26)$$

where we have defined  $p_{\pm} = p \pm q/2$ , and the quark propagators  $\tilde{S}_p^f$  in the presence of the magnetic field have been given in Eq. (12).

It is relatively easy to see that the functions  $J_{\sigma_a \pi_b}(q)$  are zero for either  $a$  or  $b$  equal to 0 or 3. However, the remaining polarization functions do not vanish in general. Since we are interested in the determination of meson masses, we consider here the particular case in which mesons are at rest, i.e. we take  $\vec{q} = 0$ ,  $q_4^2 = -m^2$ , where  $m$  stands for the corresponding meson mass. In that situation the nondiagonal polarization functions that mix the neutral scalar and vector mesons also vanish, i.e. for  $a, b = 0, 3$  one has  $\hat{J}_{\sigma_a \rho_{b\mu}} = 0$ , where the notation  $\hat{J}$  indicates that the polarization function is evaluated at the meson rest frame. In this way, the scalar meson sector gets decoupled at this level; we will not take into account these mesons in what follows. It can also be shown that  $\hat{J}_{\rho_{a\mu} \rho_{b\nu}}$ , with  $a, b = 0, 3$ , vanish for  $\mu \neq \nu$ , while the functions  $\hat{J}_{\pi_a \rho_{b\mu}}$ , with  $a, b = 0, 3$ , turn out to be proportional to  $\delta_{\mu 3}$ .

It is found that all nonvanishing polarization functions are in general divergent. As done at the MF level, we consider the magnetic field independent regularization scheme, in which we subtract the corresponding “ $B = 0$ ” contributions and then we add them in a regularized form. Thus, for a generic polarization function  $\hat{J}_{MM'}$  we have

$$\hat{J}_{MM'}^{\text{reg}} = \hat{J}_{MM'}^{0, \text{reg}} + \hat{J}_{MM'}^{\text{mag}} . \quad (27)$$

The regularized “ $B = 0$ ” pieces  $\hat{J}_{MM'}^{0,\text{reg}}$  are given in App. A; it is easy to see that all nondiagonal polarization functions  $\hat{J}_{MM'}^{0,\text{reg}}$ ,  $M \neq M'$ , are equal to zero. In the case of the “magnetic” contributions  $\hat{J}_{MM'}^{\text{mag}}$ , after a rather long calculation it is found that they can be expressed in the form given by Eq. (25), viz.

$$\hat{J}_{MM'}^{\text{mag}} = \hat{F}_{MM'}^{u,\text{mag}} + \varepsilon_M \varepsilon_{M'} \hat{F}_{MM'}^{d,\text{mag}} , \quad (28)$$

where the functions  $\hat{F}_{MM'}^{f,\text{mag}}$  are given by

$$\begin{aligned} \hat{F}_{\pi^a \pi^b}^{f,\text{mag}} &= -N_c [I_{1f}^{\text{mag}} - m^2 I_{2f}^{\text{mag}}(-m^2)] , \\ \hat{F}_{\pi^a \rho_\mu^b}^{f,\text{mag}} &= -\hat{F}_{\rho_\mu^a \pi^b}^{f,\text{mag}} = iN_c I_{3f}^{\text{mag}}(-m^2) \delta_{\mu 3} , \\ \hat{F}_{\rho_\mu^a \rho_\nu^b}^{f,\text{mag}} &= N_c [I_{4f}^{\text{mag}}(-m^2) \mathbb{1}_{\mu\nu}^\perp + m^2 I_{5f}^{\text{mag}}(-m^2) \delta_{\mu 3} \delta_{\nu 3}] , \end{aligned} \quad (29)$$

with  $\mathbb{1}^\perp = \text{diag}(1, 1, 0, 0)$ . The expression for  $I_{1f}^{\text{mag}}$  has been given in Eq. (15), whereas the integrals  $I_{nf}^{\text{mag}}$  for  $n = 2, \dots, 5$  read

$$\begin{aligned} I_{2f}^{\text{mag}}(-m^2) &= \frac{1}{8\pi^2} \int_0^1 dv \left[ \psi(\bar{x}_f) + \frac{1}{2\bar{x}_f} - \ln \bar{x}_f \right] , \\ I_{3f}^{\text{mag}}(-m^2) &= \frac{s_f M_f B_f}{\pi^2 m} \int_0^1 dv (v^2 + 4M_f^2/m^2 - 1)^{-1} , \\ I_{4f}^{\text{mag}}(-m^2) &= -I_{1f}^{\text{mag}} - \frac{m^2}{16\pi^2} \left[ \int_0^1 dv (v^2 + \gamma) \ln \bar{x}_f \right. \\ &\quad \left. - \frac{1}{2} \sum_{s=\pm 1} \int_0^1 dv (v^2 + sv/\lambda + \gamma) \psi(\bar{x}_f + (1+sv)/2) \right] , \\ I_{5f}^{\text{mag}}(-m^2) &= \frac{1}{8\pi^2} \int_0^1 dv (1-v^2) \left[ \psi(\bar{x}_f) + \frac{1}{2\bar{x}_f} - \ln \bar{x}_f \right] , \end{aligned} \quad (30)$$

where  $\lambda = m^2/(4B_f)$ ,  $\gamma = 1 + 4M_f^2/m^2$  and  $\bar{x}_f = [M_f^2 - (1-v^2)m^2/4]/(2B_f)$ . For  $m < 2M_f$  these integrals are well defined. In fact, in the case of  $I_{3f}^{\text{mag}}(-m^2)$  one can even get the analytic result

$$I_{3f}^{\text{mag}}(-m^2) = \frac{s_f B_f}{2\pi^2 \sqrt{1 - m^2/(4M_f^2)}} \arctan \left( \frac{m}{2M_f \sqrt{1 - m^2/(4M_f^2)}} \right) , \quad m < 2M_f . \quad (31)$$

In the case of  $I_{4f}^{\text{mag}}(-m^2)$ , it is worth noticing that in the limit  $m^2 \rightarrow 0$  the second term on the r.h.s. of the corresponding expression in Eqs. (30) is found to be equal to  $I_{1f}^{\text{mag}}$ . Thus, in this limit one has  $I_{4f}^{\text{mag}} \rightarrow 0$ , as it is required in order to avoid a nonzero contribution to the

photon mass coming from the “magnetic piece” of the polarization function. On the other hand, for  $m \geq 2M_f$  (i.e., beyond the  $q\bar{q}$  production threshold) the integrals are divergent. To obtain finite results we perform in this case analytic extensions. The corresponding expressions, as well as some technical details, are given in App. B.

The vector fields  $\rho_{0\mu}$  and  $\rho_{3\mu}$  can be written in a polarization vector basis. Since we assume that the mesons are at rest, we can choose polarization vectors  $\epsilon_\mu^{(S_z)}$  associated to spin projections  $S_z = 0, \pm 1$ , namely

$$\epsilon_\mu^{(0)} = (0, 0, 1, 0) , \quad \epsilon_\mu^{(1)} = \frac{1}{\sqrt{2}} (1, i, 0, 0) , \quad \epsilon_\mu^{(-1)} = \frac{1}{\sqrt{2}} (1, -i, 0, 0) . \quad (32)$$

It is convenient to distinguish between states  $\rho_{a\parallel}$  and  $\rho_{a\perp}$ , with  $a = 0, 3$ , corresponding to polarization vectors parallel and perpendicular to the magnetic field (spin projections  $S_z = 0$  and  $S_z = \pm 1$ ), respectively. From Eqs. (29) it is seen that for nonzero  $B$  pseudoscalar mesons get coupled only to neutral vector mesons with spin projection  $S_z = 0$  (in fact, this is expected from the invariance under rotations around the direction of  $\vec{B}$ ). In this way, taking into account Eq. (24) one can define a  $4 \times 4$  matrix  $G_\parallel$  with elements  $G_{MM'}$ , where  $M, M' = \pi_0, \pi_3, \rho_{0\parallel}, \rho_{3\parallel}$ , whereas for  $S_z = \pm 1$  states one gets two identical  $2 \times 2$  matrices  $G_\perp$  with elements  $G_{MM'}$ , where  $M, M' = \rho_{0\perp}, \rho_{3\perp}$ . The pole masses of  $S_z = 0$  physical mesons,  $m_\parallel^{(k)}$  (with  $k = 1, \dots, 4$ ), will be given by the solutions of

$$\det G_\parallel = 0 , \quad (33)$$

while those of the  $S_z = \pm 1$  vector mesons,  $m_\perp^{(k)}$  (with  $k = 1, 2$ ), can be obtained from

$$\det G_\perp = 0 . \quad (34)$$

Once the masses are determined, the spin-isospin composition of the physical meson states  $|k\rangle$  is given by the corresponding eigenvectors  $c^{(k)}$ . Thus, one has

$$\begin{aligned} |k\rangle &= c_{\pi_0}^{(k)} |\pi_0\rangle + c_{\pi_3}^{(k)} |\pi_3\rangle + i c_{\rho_{0\parallel}}^{(k)} |\rho_{0\parallel}\rangle + i c_{\rho_{3\parallel}}^{(k)} |\rho_{3\parallel}\rangle , \quad k = 1, \dots, 4 && \text{for } S_z = 0 \text{ states} , \\ |k\rangle &= c_{\rho_{3\perp}}^{(k)} |\rho_{0\perp}\rangle + c_{\rho_{3\perp}}^{(k)} |\rho_{3\perp}\rangle , \quad k = 1, 2 && \text{for } S_z = \pm 1 \text{ states} . \end{aligned} \quad (35)$$

It is also useful to consider the flavor basis  $\pi_f, \rho_f$ , where  $f = u, d$ . Isospin states can be written in terms of flavor states using the relations

$$\begin{aligned} |\pi_0\rangle &= \frac{1}{\sqrt{2}} (|\pi_u\rangle + |\pi_d\rangle) , & |\pi_3\rangle &= \frac{1}{\sqrt{2}} (|\pi_u\rangle - |\pi_d\rangle) , \\ |\rho_{0\parallel}\rangle &= \frac{1}{\sqrt{2}} (|\rho_{u\parallel}\rangle + |\rho_{d\parallel}\rangle) , & |\rho_{3\parallel}\rangle &= \frac{1}{\sqrt{2}} (|\rho_{u\parallel}\rangle - |\rho_{d\parallel}\rangle) . \end{aligned} \quad (36)$$

In the  $S_z = \pm 1$  sector, where there is no mixing between pseudoscalar and vector mesons, the states  $|\rho_{u\perp}\rangle$  and  $|\rho_{d\perp}\rangle$  turn out to be the mass eigenstates that diagonalize  $G_\perp$ . This can be easily understood noticing that the external magnetic field distinguishes between quarks that carry different electric charges, and this is what breaks the  $u$ - $d$  flavor degeneracy. In the flavor basis one has  $G_\perp = \text{diag}(G_{u\perp}, G_{d\perp})$ , where

$$G_{f\perp}(-m^2) = \frac{1}{2g_v} + \frac{4N_c}{3} \left[ (2M_f^2 + m^2) I_{2f}(-m^2) - 2M_f^2 I_{2f}(0) \right] + 2N_c I_{4f}^{\text{mag}}(-m^2), \quad (37)$$

where the expression for  $I_{2f}(q^2)$  can be found in App. A, and  $I_{4f}^{\text{mag}}(-m^2)$  has been given in Eqs. (30). A similar situation occurs in the  $S_z = 0$  sector if one has  $\alpha = 0$ . In this particular case there is no flavor mixing either in the pseudoscalar or vector meson sectors, hence the  $4 \times 4$  matrix  $G_\parallel$  can be written as a direct sum of  $2 \times 2$  flavor matrices  $G_{u\parallel}$  and  $G_{d\parallel}$ . Moreover, for a given value of  $B$ , the meson masses of e.g.  $u$ -like mesons (solutions of the equation  $\det G_{u\parallel} = 0$ ) can be obtained from those of  $d$ -like mesons for  $B' = 2B$ , since  $|Q_u| = 2|Q_d|$  and  $\det G_{f\parallel}$  depends on  $Q_f$  and  $B$  only through the combination  $B_f = |Q_f B|$  (this also holds for the implicit dependence on  $Q_f$  and  $B$  through the quark effective masses  $M_f$ ). If one has  $\alpha \neq 0$  this relation is no longer valid, and in general  $G_\parallel$  cannot be separated into flavor pieces. In fact, as we discuss below, in the pseudoscalar sector it is seen that chiral symmetry largely dominates over flavor symmetry; for the range of values of  $B$  considered in this work, we find that even for  $\alpha \ll 1$  the lightest  $S_z = 0$  mass eigenstates are very close to isospin states  $\pi_3$  and  $\pi_0$ , instead of approximating to flavor states  $\pi_f$ .

### III. NUMERICAL RESULTS

#### A. Model parametrization and mean field results

To obtain numerical results for the dependence of meson masses on the external magnetic field, one first has to fix the parameters of the model. Here we take the parameter set  $m_c = 5.833$  MeV,  $\Lambda = 587.9$  MeV and  $g\Lambda^2 = 2.44$ , which —for vanishing external field— lead to effective quark masses  $M_f = 400$  MeV and quark-antiquark condensates  $\phi_f^0 = (-241 \text{ MeV})^3$ , for  $f = u, d$ . This parametrization properly reproduces the empirical values of the pion mass and decay constant in vacuum, namely  $m_\pi = 138$  MeV and  $f_\pi = 92.4$  MeV. Regarding the vector couplings, we take  $g_{v_3} = 2.651/\Lambda^2$ , which leads to  $m_\rho = 770$  MeV at  $B = 0$ , and  $g_{v_0} = g_{v_3}$ , which is consistent with the fact that  $m_\rho \simeq m_\omega$  at vanishing external field. For

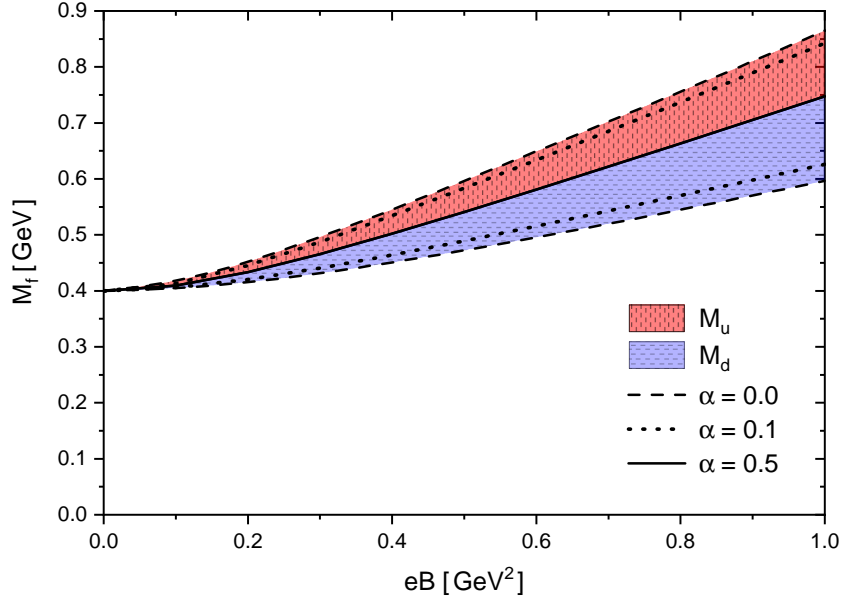


Figure 1. (Color online) Effective quark masses  $M_u$  (red upper band),  $M_d$  (blue lower band) as functions of  $eB$ . The extremes of the bands correspond to  $\alpha = 0$  (dashed lines) and  $\alpha = 0.5$  (full line). The dotted lines correspond to  $\alpha = 0.1$ .

these constants we use from now on the notation  $g_v \equiv g_{v_0} = g_{v_3}$ . Finally, as stated in Sec. II A, the amount of flavor mixing induced by the 't Hooft-like interaction is controlled by the parameter  $\alpha$ . In this work we choose to take as a reference value  $\alpha = 0.1$ , since it leads (at  $B = 0$ ) to an approximate  $\eta$  meson mass  $m_\eta \simeq 520$  MeV, in reasonable agreement with the physical value  $m_\eta^{\text{phys}} = 548$  MeV. In fact, this mass is very sensitive to minor changes in  $\alpha$ . An alternative estimate for this parameter can be obtained from the  $\eta - \eta'$  mass splitting within the 3-flavor NJL model [73], which leads to  $\alpha \simeq 0.2$  [74]. In any case, to obtain a full understanding of the effects of flavor mixing we will also consider the values  $\alpha = 0$  and  $\alpha = 0.5$ , corresponding to the situation in which flavors are decoupled and in which there is full flavor mixing, respectively. It is easily seen that for  $\alpha = 0$  the  $\pi$  and  $\eta$  mesons have equal (finite) masses, while when  $\alpha$  approaches 0.5 the mass of the pion stays finite and that of the  $\eta$  meson becomes increasingly large.

In Fig. 1 we show the numerical results obtained for the magnetic field dependence of the dynamical quark masses  $M_u$  and  $M_d$ . Both masses are found to get increased with  $B$ , and

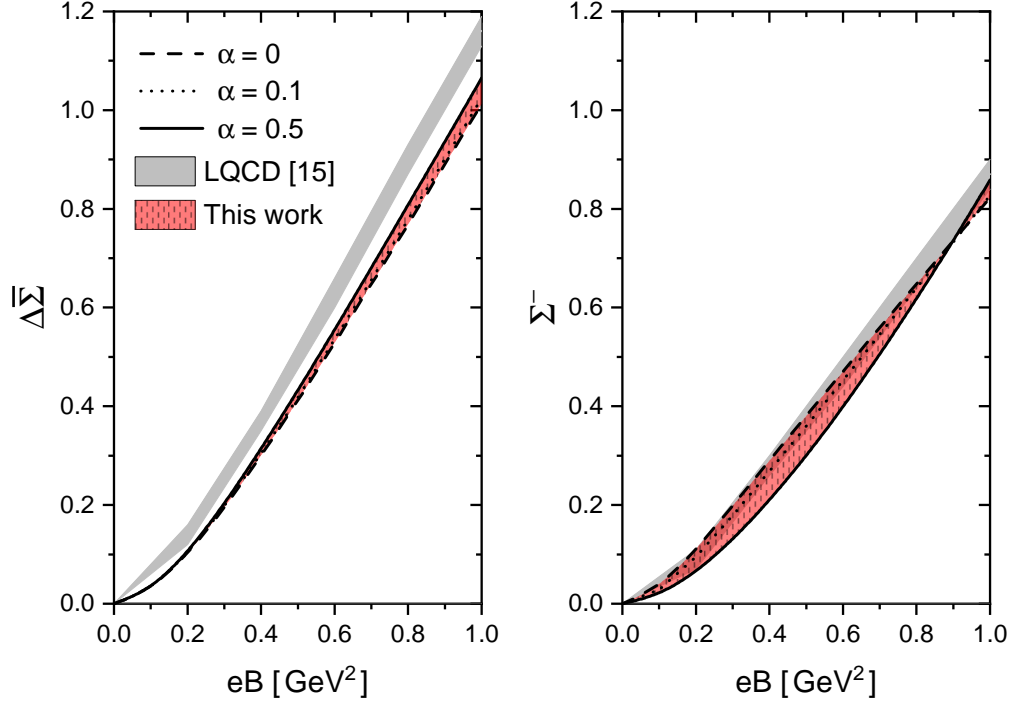


Figure 2. (Color online) Normalized average condensate (left) and normalized condensate difference (right) as functions of  $eB$ , for values of  $\alpha$  from 0 to 1 (see text for definitions). LQCD results from Ref. [16] (gray bands) are added for comparison.

it is seen that for  $M_u$  ( $M_d$ ) the slope becomes larger (smaller) as  $\alpha$  decreases from  $\alpha = 0.5$  —where both masses coincide— to  $\alpha = 0$ . Next, in Fig. 2, we show the dependence of normalized light quark-antiquark condensates on  $B$ . Following Ref. [16], we introduce the definitions

$$\Delta\bar{\Sigma} = \frac{\Delta\Sigma_u + \Delta\Sigma_d}{2} \quad , \quad \Sigma^- = \Delta\Sigma_u - \Delta\Sigma_d \quad , \quad (38)$$

where  $\Delta\Sigma_f = -2m_c[\phi_f(B) - \phi_f^0]/D^4$ ,  $D = (135 \times 86)^{1/2}$  MeV being a phenomenological normalization constant. In the left and right panels of Fig. 2 we plot the values of  $\Delta\bar{\Sigma}$  and  $\Sigma^-$ , respectively, as functions of  $eB$ . The gray bands correspond to LQCD values taken from Ref. [16], whereas the red bands cover our results for the range  $\alpha = 0$  to  $\alpha = 0.5$ . We observe from this figure that the model reproduces properly the zero-temperature magnetic catalysis found in LQCD calculations. Moreover, it is seen that the dependence on the flavor mixing parameter  $\alpha$  is rather mild.

## B. Pseudoscalar and $S_z = 0$ vector meson sector

In this subsection we present and discuss the results associated with the coupled system composed by neutral pseudoscalar mesons and  $S_z = 0$  neutral vector mesons. As discussed in Sec. II B, the corresponding masses  $m_{\parallel}^{(k)}$ ,  $k = 1, \dots, 4$ , can be obtained from Eq. (33). The dependence of these masses with the magnetic field for the reference value  $\alpha = 0.1$  are shown in Fig. 3. As discussed below, the spin-isospin compositions of the associated states do not coincide in general with those of the usual  $B = 0$  states  $\pi^0$ ,  $\eta$ ,  $\rho^0$  and  $\omega$ . For this reason, we use for these states the notation  $\tilde{M}$ , where in each case  $M$  is the state that has the larger weight  $c_M^{(k)}$  in the spin-isospin decomposition given by Eq. (35) (see Table I). In Fig. 3 we also

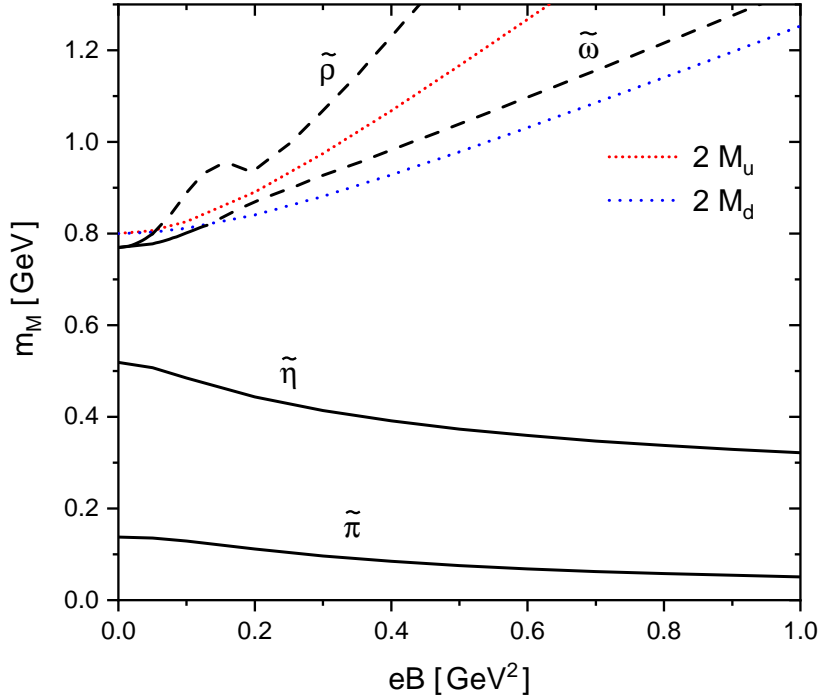


Figure 3. (Color online) Masses of  $S_z = 0$  mesons as functions of  $eB$ , for  $\alpha = 0.1$ . The dotted lines indicate  $u\bar{u}$  and  $d\bar{d}$  production thresholds.

show the  $q\bar{q}$  production thresholds  $m = 2M_d$  and  $m = 2M_u$  (dotted and short-dotted lines, respectively), beyond which some of the matrix elements of  $G_{\parallel}$  get absorptive parts. The presence of these absorptive parts implies that for the states  $\tilde{\rho}$  and  $\tilde{\omega}$  there are certain values of the magnetic field above which the associated particles are unstable with respect to an

unphysical decay into a  $q\bar{q}$  pair. In fact, the existence of such decays is a well known feature of the NJL model, even in the absence of an external field [60–62]; it arises as a consequence of the lack of a confinement mechanism, which is a characteristic of this type of model. In the presence of the magnetic field, one also has to deal with new poles that may arise from the thresholds related to the Landau level decomposition of the intermediate quark propagators. As customary, we will assume that the widths associated to these unphysical decays are small. Then, to determine the values of the corresponding masses, we consider an extremum condition for the meson propagators, similar to the method discussed e.g. in Ref. [75]. It has to be kept in mind, however, that these predictions for the meson masses are less reliable in comparison to those obtained for the states lying below the quark pair production threshold, and should be taken just as qualitative results. For this reason, in Fig. 3 we use dashed lines to plot  $\tilde{\rho}$  and  $\tilde{\omega}$  masses above the  $2M_d$  threshold.

It is interesting at this stage to discuss the spin-isospin composition of mass states and their variation with the external field. As mentioned at the end of Sec. IIB, the magnetic field tends to separate the states according to the charges of the quark components. In the case  $\alpha = 0$ , although there is no flavor mixing, flavor degeneracy gets broken due to the magnetic field. Therefore, mass eigenstates turn out to be separated into particles with pure  $u$  or  $d$  quark content. If we use the labels  $k = 1, 3$  and  $k = 2, 4$  for “ $u$ ” and “ $d$ ” states respectively, we get [see Eqs. (36)]

$$\begin{aligned} |k\rangle &= c_{\pi_u}^{(k)} |\pi_u\rangle + i c_{\rho_{u\parallel}}^{(k)} |\rho_{u\parallel}\rangle = \frac{c_{\pi_u}^{(k)}}{\sqrt{2}} |\pi_0\rangle + \frac{c_{\pi_u}^{(k)}}{\sqrt{2}} |\pi_3\rangle + i \frac{c_{\rho_{u\parallel}}^{(k)}}{\sqrt{2}} |\rho_{0\parallel}\rangle + i \frac{c_{\rho_{u\parallel}}^{(k)}}{\sqrt{2}} |\rho_{3\parallel}\rangle, \quad k = 1, 3, \\ |k\rangle &= c_{\pi_d}^{(k)} |\pi_d\rangle + i c_{\rho_{d\parallel}}^{(k)} |\rho_{d\parallel}\rangle = \frac{c_{\pi_d}^{(k)}}{\sqrt{2}} |\pi_0\rangle - \frac{c_{\pi_d}^{(k)}}{\sqrt{2}} |\pi_3\rangle + i \frac{c_{\rho_{d\parallel}}^{(k)}}{\sqrt{2}} |\rho_{0\parallel}\rangle - i \frac{c_{\rho_{d\parallel}}^{(k)}}{\sqrt{2}} |\rho_{3\parallel}\rangle, \quad k = 2, 4. \end{aligned} \quad (39)$$

For definiteness, let us take  $m_{\parallel}^{(1)} < m_{\parallel}^{(3)}$ ,  $m_{\parallel}^{(2)} < m_{\parallel}^{(4)}$ . Since for  $\alpha = 0$  and  $B = 0$  the Lagrangian shows an approximate symmetry under  $SU(2)_A \otimes U(1)_A$  chiral transformations, spontaneous symmetry breaking leads to four pseudo-Goldstone bosons, viz. the three pions and the  $\eta$  meson. In the presence of the magnetic field, chiral symmetry is explicitly broken from  $SU(2)_A \otimes U(1)_A$  down to  $U(1)_{T^3, A} \otimes U(1)_A$ ; thus, one still has two neutral mesons—combinations of the neutral pion and the  $\eta$ —that remain as pseudo-Goldstone bosons. Moreover, according to the previous discussion, the latter must be pure  $u$  and  $d$ -states. Since they should be approximate mass eigenstates, one expects to find  $(c_{\pi_u}^{(1)}, c_{\rho_{u\parallel}}^{(1)}) \approx (c_{\pi_d}^{(2)}, c_{\rho_{d\parallel}}^{(2)}) \approx (1, 0)$  and  $(c_{\pi_u}^{(3)}, c_{\rho_{u\parallel}}^{(3)}) \approx (c_{\pi_d}^{(4)}, c_{\rho_{d\parallel}}^{(4)}) \approx (0, 1)$ . On the other hand, for  $\alpha \neq 0$  the presence of



the 't Hooft term introduces flavor mixing at the level of scalar and pseudoscalar four-quark interactions, breaking the  $U(1)_A$  symmetry. Thus, the spin-isospin decomposition gets the more general form given in Eq. (35), where the lightest state can still be identified as an approximate Goldstone boson. When  $\alpha$  approaches 0.5, the  $\tilde{\eta}$  mass goes to infinity and, accordingly, the  $|\pi_0\rangle$  component in Eq. (35) disappears from the remaining states.

In Table I we quote the composition of the mass eigenstates  $\tilde{M}$  described in Fig. 3, for some representative values of the magnetic field. For completeness, the coefficients corresponding to both spin-isospin and spin-flavor basis are included. We note that while the mass eigenvalues do not depend on whether  $B$  is positive or negative, the corresponding eigenvectors do. The relative signs in Table I correspond to the choice  $B > 0$ .

State	$eB$ [GeV <sup>2</sup> ]	Spin-isospin composition				Spin-flavor composition			
		$c_{\pi_0}^{(k)}$	$c_{\pi_3}^{(k)}$	$c_{\rho_{0  }}^{(k)}$	$c_{\rho_{3  }}^{(k)}$	$c_{\pi_u}^{(k)}$	$c_{\pi_d}^{(k)}$	$c_{\rho_{u  }}^{(k)}$	$c_{\rho_{d  }}^{(k)}$
$\tilde{\pi}$ ( $k = 1$ )	0.05	0.0037	0.9998	-0.0203	-0.0068	0.7096	-0.7043	-0.0192	-0.0095
	0.5	0.1019	0.9910	-0.0822	-0.0285	0.7728	-0.6287	-0.0783	-0.038
	1.0	0.1566	0.9841	-0.0797	-0.0274	0.8066	-0.5851	-0.0757	-0.037
$\tilde{\eta}$ ( $k = 2$ )	0.05	0.9899	-0.0413	-0.0381	-0.1301	0.6708	0.7292	-0.1189	0.0651
	0.5	0.8661	-0.3246	0.0582	-0.3757	0.3829	0.8420	-0.2245	0.3068
	1.0	0.8353	-0.3445	0.1048	-0.4154	0.3470	0.8342	-0.2196	0.3678
$\tilde{\omega}$ ( $k = 3$ )	0.05	-0.1979	0.2693	0.7601	-0.5572	0.0505	-0.3304	0.1435	0.9315
$\tilde{\rho}$ ( $k = 4$ )	0.05	0.4925	0.3312	0.4685	0.6544	0.5824	0.1141	0.7940	-0.1315

Table I. Composition of the  $S_z = 0$  meson mass eigenstates for some selected values of  $eB$ . Results correspond to  $\alpha = 0.1$ . Relative signs hold for the choice  $B > 0$ .

Let us first discuss the composition of the  $\tilde{\pi}$  state ( $k = 1$ ), which is the one that has the lowest mass. We see that even though  $\alpha$  is relatively small, the effect of flavor mixing is already very strong; the spin-isospin composition is clearly dominated by the  $\pi_3$  component, which is given by an antisymmetric equal-weight combination of  $u$  and  $d$  quark flavors. Thus, the mass states are far from satisfying the flavor disentanglement expected for the case  $\alpha = 0$  [see Eqs. (39)], in which one has two approximate Goldstone bosons. In fact, once  $\alpha$  is turned on, explicitly breaking the  $U(1)_A$  symmetry,  $\pi_3$  is the only state that remains

being a pseudo-Goldstone boson; this forces the lowest-mass state  $\tilde{\pi}$  to be dominated by the  $\pi_3$  component. As discussed above, the presence of the magnetic field distinguishes between flavor components  $\pi_u$  and  $\pi_d$  instead of isospin states. However, it is found that even for values of  $\alpha$  as small as 0.01 the mass state  $\tilde{\pi}$  is still dominated by the  $\pi_3$  component ( $|c_{\pi_3}^{(1)}|^2 \gtrsim 0.9$ ) for the full range of values of  $eB$  considered here. In other words, extremely large magnetic fields would be required in order to rule the composition of light mass eigenstates, which is otherwise dictated by the invariance under  $U(1)_{T^3, A}$  transformations. Coming back to the case  $\alpha = 0.1$ , we see that, although relatively small, the effect of the magnetic field on the composition of the  $\tilde{\pi}$  state can be observed from the values in Table I. When  $eB$  gets increased, it is found that there is a slight decrease of the component  $\pi^3$  in favor of the others. In addition, a larger weight is gained by the  $u$ -flavor components, as one can see by looking at the entries corresponding to the spin-flavor states (last four columns of Table I): one has  $|c_{\pi_u}^{(1)}|^2 + |c_{\rho_{u\parallel}}^{(1)}|^2 = 0.50(0.66)$  for  $eB = 0.05(1.0)$  GeV<sup>2</sup>. This can be understood noticing that the magnetic field is known to reduce the mass of the lowest neutral meson state [49, 52, 53]. Thus, for large  $eB$  it is expected that  $\tilde{\pi}$  will have a larger component of the quark flavor that couples strongly to the magnetic field (i.e., the  $u$  quark). Concerning the vector meson components of the  $\tilde{\pi}$  state, it is seen that they are completely negligible at low values of  $eB$ , reaching a contribution  $|c_{\rho_{u\parallel}}^{(1)}|^2 + |c_{\rho_{d\parallel}}^{(1)}|^2 \simeq 0.01$  (i.e., about 1%) at  $eB = 1$  GeV<sup>2</sup>.

Turning now to the composition of the  $\tilde{\eta}$  state ( $k = 2$ ) in Table I, we see that, as expected from the above discussion, it is dominated by the  $\pi^0$  ( $I = 0$ ) component for values of  $eB$  up to 1 GeV<sup>2</sup>. Regarding the flavor composition, in this case the  $d$ -quark content is the one that increases as  $eB$  does, with  $|c_{\pi_d}^{(2)}|^2 + |c_{\rho_{d\parallel}}^{(2)}|^2 = 0.54(0.70)$  for  $eB = 0.05(1.0)$  GeV<sup>2</sup>. Now the weight of the vector components is larger than in the case of the  $\tilde{\pi}$  state,  $|c_{\rho_{u\parallel}}^{(1)}|^2 + |c_{\rho_{d\parallel}}^{(1)}|^2$  ranging from 0.02 at  $eB = 0.05$  GeV<sup>2</sup> to 0.17 at  $eB = 1.0$  GeV<sup>2</sup>. This is probably due to the fact that for  $\alpha = 0.1$  the  $\tilde{\eta}$  mass is closer to vector meson masses.

Finally, let us comment on the composition of the  $\tilde{\omega}$  and  $\tilde{\rho}$  states ( $k = 3$  and  $k = 4$ , respectively). As mentioned above, the masses of these states reach the threshold for  $q\bar{q}$  decay for rather low values of the magnetic field, hence our predictions for these quantities should be taken as qualitative ones for a major part of the  $eB$  range considered here. It is worth noticing that there is a multiple number of thresholds, which get successively opened each time the meson mass is sufficiently large so that the quark and antiquark meson components can populate a new Landau level. The first thresholds in the  $\bar{u}u$  and the  $\bar{d}d$  sectors are

reached at meson masses equal to  $2M_u$  and  $2M_d$ , respectively. It is important to realize that they do not correspond to a free quark together with a free antiquark, but to the quark and antiquark in their lowest Landau levels. Taking  $B > 0$ , if both the quark and the antiquark have vanishing  $z$  component of the momentum, the corresponding spin configurations are  $u (S_z = +\frac{1}{2}) \bar{u} (S_z = -\frac{1}{2})$  and  $d (S_z = -\frac{1}{2}) \bar{d} (S_z = +\frac{1}{2})$ . In both cases, the magnetic dipole moments of the quark and the antiquark are parallel to the magnetic field; the difference between both configurations arises from the opposite signs of the quark electric charges. We only quote in Table I the  $\tilde{\omega}$  and  $\tilde{\rho}$  compositions in the presence of a low magnetic field  $eB = 0.05 \text{ GeV}^2$ , for which the masses of both states are below the  $2M_f$  threshold and the values of the coefficients  $c_M^{(k)}$  should be more reliable. Interestingly, we note that even at this low value of the magnetic field the composition of the vector meson mass states is clearly flavor-dominated: from Table I one has  $|c_{\pi_d}^{(3)}|^2 + |c_{\rho_{d\parallel}}^{(3)}|^2 = 0.98$ ,  $|c_{\pi_u}^{(4)}|^2 + |c_{\rho_{u\parallel}}^{(4)}|^2 = 0.97$ . Thus, whereas for no external field one usually identifies the (approximately degenerate) mass states as isospin eigenstates  $\rho^0$  and  $\omega$ , in the presence of the magnetic field the states  $\tilde{\rho}$  and  $\tilde{\omega}$  are closer to a  $\rho_{u\parallel}$  and a  $\rho_{d\parallel}$ , rather than a  $\rho_{3\parallel}$  and a  $\rho_{0\parallel}$ . In fact, given the symmetry of the vector-like interactions in the Lagrangian in Eq. (1), the small deviation of  $\tilde{\rho}$  and  $\tilde{\omega}$  from pure flavor states can be attributed to the mixing with the pseudoscalar sector, where isospin states are dominant. Notice that although the vector components are larger than the pseudoscalar ones, the weight of the latter is not negligible, specially for the  $\tilde{\rho}$  state (which is the one with a larger mass, as shown in Fig. 3), with  $|c_{\pi_u}^{(4)}|^2 + |c_{\rho_u}^{(4)}|^2 \simeq 0.35$ . This can be understood from an analysis similar to the one performed for the meson mass thresholds in terms of the quark spins. A larger content of the  $d (S_z = -\frac{1}{2}) \bar{d} (S_z = +\frac{1}{2})$  component has to be expected in the case of the  $\tilde{\omega}$ , while there should be a larger content of the  $u (S_z = +\frac{1}{2}) \bar{u} (S_z = -\frac{1}{2})$  one in the case of the  $\tilde{\rho}$ . From Table I it is seen that these combinations correspond to  $(c_{\pi_d}^{(3)} - c_{\rho_{d\parallel}}^{(3)})/\sqrt{2} = -0.89$  for the  $\tilde{\omega}$  and  $(c_{\pi_u}^{(4)} + c_{\rho_{u\parallel}}^{(4)})/\sqrt{2} = 0.97$  for the  $\tilde{\rho}$ , under a magnetic field as low as  $eB = 0.05 \text{ GeV}^2$ —and this effect should be more significant for larger values of  $eB$ .

We analyze in what follows the impact of both flavor mixing and pseudoscalar-vector mixing on the masses of the lightest states. In fact, this is one of the main issues of this work. In Fig. 4 we show the  $B$  dependence of light meson masses with (dashed lines) and without (dotted lines) pseudoscalar-vector mixing, considering three representative values of the flavor-mixing constant  $\alpha$ . The results without pseudoscalar-vector mixing are obtained

just by setting to zero the off-diagonal polarization functions  $\hat{J}_{\pi_a \rho_{b\mu}}^{\text{mag}}$  and  $\hat{J}_{\rho_{a\mu} \pi_b}^{\text{mag}}$  in Eq. (27). Let us focus on  $m_{\tilde{\pi}}$ , considering first the effect of varying  $\alpha$ ; as can be seen from Fig. 4, this effect is rather independent of whether pseudoscalar states mix with vectors or not. We

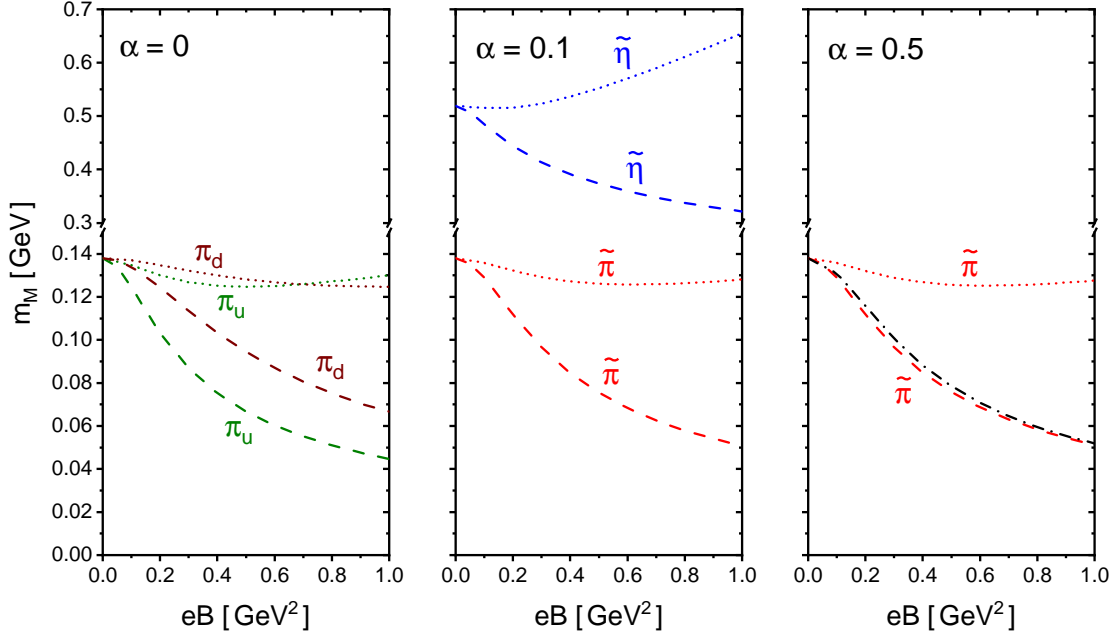


Figure 4. (Color online) Masses of the lightest  $S_z = 0$  mesons as functions of  $eB$ , for various values of  $\alpha$ . Dashed (dotted) lines correspond to the case in which the mixing between pseudoscalar and vector states is (is not) included. The dash-dotted line in the right panel is obtained from the approximate expression in Eq. (40).

observe that for  $\alpha = 0$  (no flavor mixing) there are two light mesons having similar masses; as stated above, these are pure flavor states and can be identified as approximate Goldstone bosons. For  $\alpha \neq 0$ , the mass of the  $\tilde{\pi}$  state is still protected owing to its pseudo-Goldstone boson character, whereas the  $\tilde{\eta}$  state becomes heavier when  $\alpha$  gets increased, and disappears from the spectrum in the limit  $\alpha = 0.5$ .

From Fig. 4 it is also seen that, for all values of  $\alpha$ , the mixing between pseudoscalar and vector meson states produces a significant decrease in the mass of the lightest state. This might be surprising, since —as shown above— the vector meson components of the  $\tilde{\pi}$  state are found to be very small even for large values of  $eB$ . The explanation of this puzzle is

discussed in detail in App. C, where it is shown that these two facts are indeed consistent. Moreover, for  $\alpha = 0.5$  it is shown that if the pseudoscalar-vector meson mixing is treated perturbatively, one can derive a simple formula for the  $B$  dependence of the  $\tilde{\pi}$  mass, viz.

$$m_{\tilde{\pi}} = \frac{\bar{m}_{\tilde{\pi}}}{\sqrt{1 + \kappa (\bar{m}_{\tilde{\pi}} eB)^2 / M_f}} , \quad (40)$$

where  $\kappa = 5N_c^2 g g_v / (18\pi^4 m_c)$ ,  $f$  is either  $u$  or  $d$ , and  $\bar{m}_{\tilde{\pi}}$  stands for the  $\tilde{\pi}$  mass when no mixing is considered. Taking into account that  $\bar{m}_{\tilde{\pi}}$  is very weakly dependent on  $B$  (see dotted lines in Fig. 4), it follows that  $m_{\tilde{\pi}}$  basically depends on the magnetic field through the ratio  $(eB)^2 / M_f$ . Notice that the  $B$  dependence of  $M_f$  for  $\alpha = 0.5$  is represented by the solid line in Fig. 1. The numerical results for  $m_{\tilde{\pi}}$  from Eq. (40), within the approximation  $\bar{m}_{\tilde{\pi}} = m_{\pi}(B = 0)$  [see Eq. (C9)] are indicated by the black dash-dotted line in the right panel (corresponding to  $\alpha = 0.5$ ) of Fig. 4. It can be seen that they are in excellent agreement with those obtained from the full calculation.

To conclude this subsection, in Fig. 5 we compare our results for the mass of the  $\tilde{\pi}$  state with those obtained in LQCD calculations, reported in Ref. [52] (quenched Wilson fermions), Ref. [53] (improved staggered quarks) and Refs. [15, 52, 76] (dynamical staggered quarks). We first note that in those calculations the authors neglect disconnected diagrams as well as the associated mixing, and work with the individual flavor states instead. In our calculation this can be achieved by setting  $\alpha = 0$ . In any case, as seen from the above analysis, the mass of the lightest meson is approximately independent of the value of  $\alpha$ ; therefore, it is reasonable to compare the mentioned LQCD results with those obtained using the reference value  $\alpha = 0.1$  that leads to an acceptable value for the  $\eta$  meson mass at vanishing external field. We also note that LQCD results have been obtained using different methods and values of the pion mass at  $B = 0$ . In particular, the most recent ones (i.e. those in Ref. [53]) are based on a highly improved staggered quark action that uses  $m_{\pi}(B = 0) = 220$  MeV, while the calculations in Refs. [15, 52, 76] take the physical value of  $m_{\pi}$  within a staggered simulation setup. Anyway, in our model we see that when the pseudoscalar-vector meson mixing is included, the values for the  $\tilde{\pi}$  meson mass lie in general below LQCD predictions. We have checked that this general result is quite insensitive to a reasonable variation of the model parameters. In addition, we have verified that the situation does not change significantly if the  $B = 0$  expressions are regularized using the Pauli-Villars scheme, as proposed e.g. in Ref. [57].

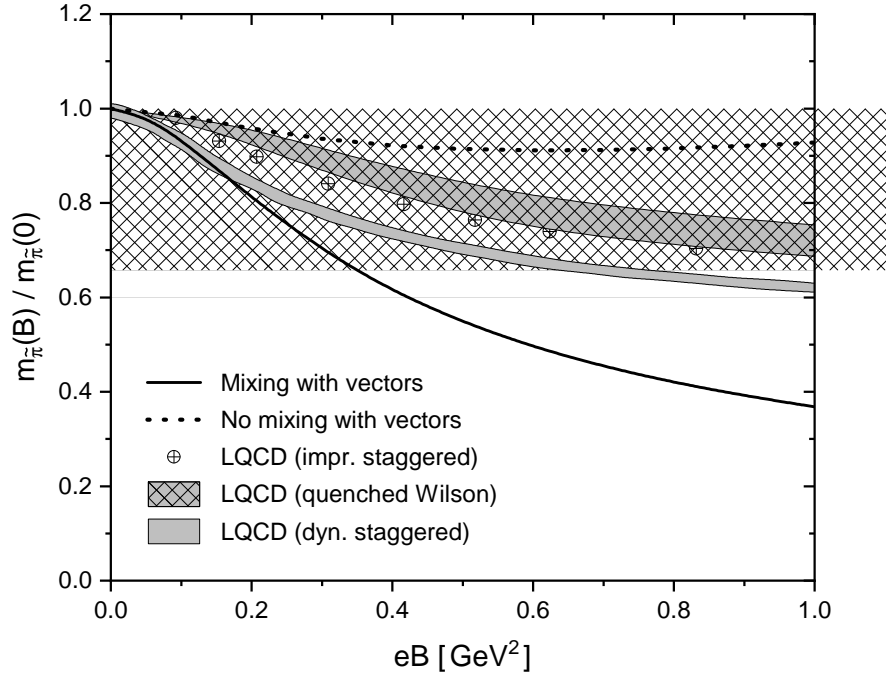


Figure 5. Normalized mass of the  $\tilde{\pi}$  meson (lightest state of the  $S_z = 0$  sector) as a function of  $eB$ , compared with LQCD results quoted in Ref. [52] (quenched Wilson fermions), Ref. [53] (improved staggered quarks) and Refs. [15, 52, 76] (dynamical staggered quarks). Solid and dotted lines correspond to NJL results with and without pseudoscalar-vector meson mixing, respectively.

### C. $S_z = \pm 1$ vector meson sector

In this subsection we present the numerical results associated with the coupled system composed by the neutral vector mesons with  $|S_z| = 1$ . As discussed in Sect. II B, for any value of  $\alpha$  the mass eigenstates can be identified according to their flavor content,  $|\rho_{u\perp}\rangle$  and  $|\rho_{d\perp}\rangle$ . The corresponding masses can be obtained by solving the equations  $G_{f\perp}(-m_{\rho_{f\perp}}^2) = 0$ , for  $f = u, d$ , with  $G_{f\perp}(-m^2)$  given by Eq. (37).

The numerical results for the meson masses as functions of the magnetic field for the case  $\alpha = 0.1$  are shown in Fig. 6, where it is seen that both  $m_{\rho_{u\perp}}$  and  $m_{\rho_{d\perp}}$  get increased with  $B$ . The enhancement is larger in the case of the  $\rho_{u\perp}$  mass; this can be understood from the larger (absolute) value of the  $u$ -quark charge, which measures the coupling with the magnetic field. As in the case of  $S_z = 0$  mesons, there are multiple mass thresholds for  $q\bar{q}$  pair production

[see Eqs. (B4) and (B7)]. The lowest one, reached at  $m_{\rho_{f\perp}} = m_f^- = M_f + \sqrt{M_f^2 + 2B_f}$ , corresponds now to the situation in which *both* the spins of the quark and the antiquark components of the  $\rho_{f\perp}$  are aligned (or anti-aligned) with the magnetic field. Notice that in this case one of the fermions lies in its lowest Landau level, while the other one is in the first excited Landau level; whether both particle spins are aligned or anti-aligned with the magnetic field depends on the signs of  $S_z$  and  $B$ . It can be seen that the values of  $m_f^-$  for  $f = u$  or  $d$  are not surpassed by the corresponding meson masses  $m_{\rho_{f\perp}}$  in the studied region, and consequently these masses are found to be smooth real functions of  $eB$ , as shown in Fig. 6. We stress that the mass values  $m = 2M_u$  and  $m = 2M_d$  are not actual thresholds in this case, since —as discussed above— they correspond to lowest Landau level quark configurations that lead to  $S_z = 0$  meson states. The absence of these thresholds can be formally shown by looking at the expression in Eq. (37); it can be seen that although the functions  $I_{2f}(-m^2)$  and  $I_{4f}^{\text{mag}}(-m^2)$  become complex for  $m > 2M_f$ , imaginary parts cancel each other and one ends up with a vanishing absorptive contribution.

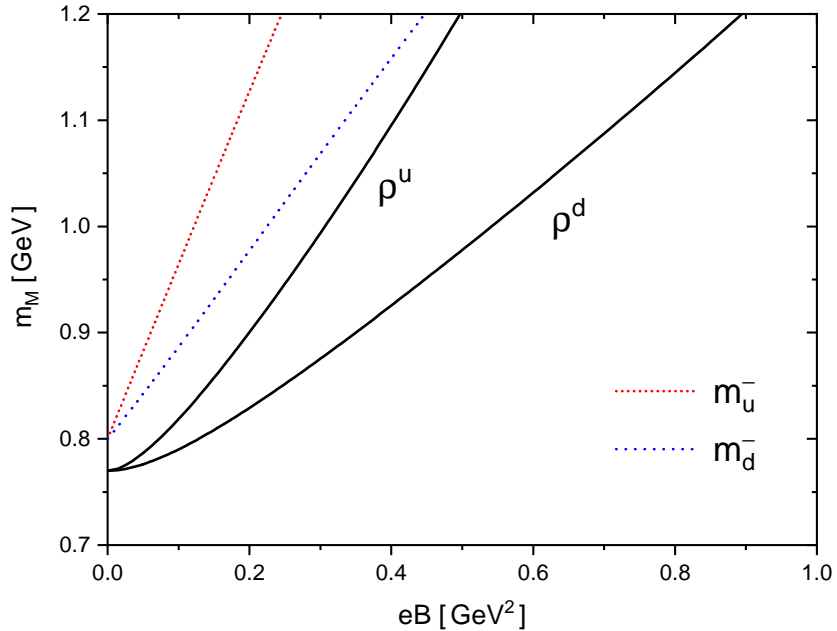


Figure 6. (Color online) Masses of the  $S_z = \pm 1$  vector meson states as functions of  $eB$ . Dotted and short-dotted lines indicate  $m_d^-$  and  $m_u^-$  quark-antiquark production thresholds, respectively.

It should be pointed out that even though there is no direct flavor mixing in this sector,

$\rho_{u\perp}$  and  $\rho_{d\perp}$  meson masses still depend on  $\alpha$ . This is due to the fact that the values of  $M_u$  and  $M_d$  obtained at the MF level get modified by flavor mixing. We recall that  $M_u(eB) = M_d(2eB)$  for  $\alpha = 0$ , while for  $\alpha = 0.5$  one has  $M_u(eB) = M_d(eB)$ . The effect of flavor mixing is illustrated in Fig. 7, where we show the  $B$  dependence of  $\rho_{u\perp}$  and  $\rho_{d\perp}$  meson masses for  $\alpha = 0, 0.1$  and  $0.5$ . As expected from the aforementioned relations between  $M_u$  and  $M_d$ , it is seen that the curves for both masses tend to become more similar as  $\alpha$  increases. However, the overall effect is found to be relatively weak. As a reference we also plot (full black line) the situation in which the mixing between  $S_z = \pm 1$  vector states is neglected, and, therefore, the masses of both states coincide. We see that even in the case  $\alpha = 0.5$  there is a certain non-negligible repulsion between states when the mixing term is turned on.

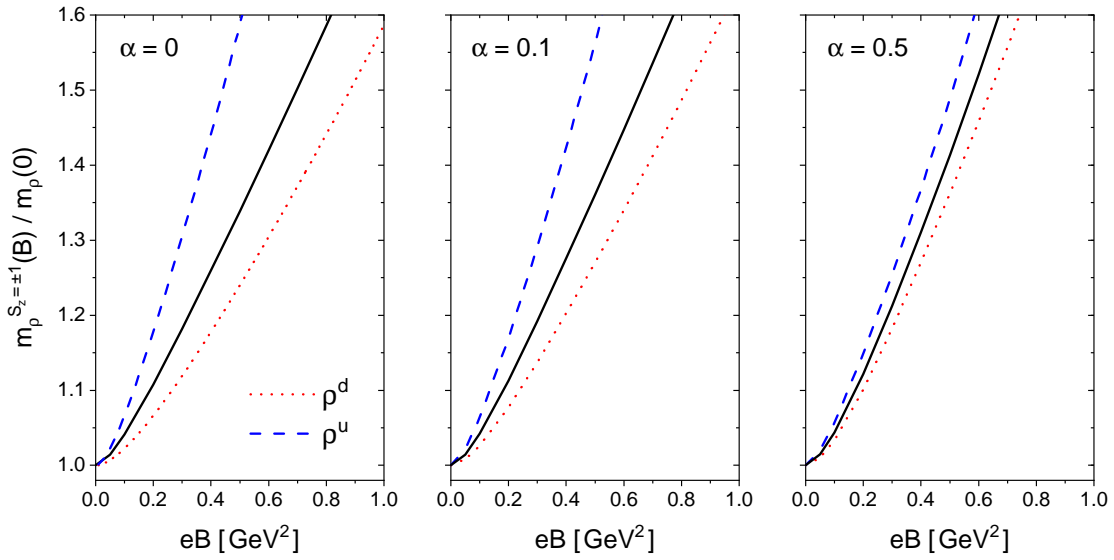


Figure 7. (Color online) Masses of  $S_z = \pm 1$  vector mesons as functions of  $eB$ , for various values of  $\alpha$ . The full black lines correspond to the case in which the mixing between pseudoscalar and vector meson states is not considered.

It is also interesting at this stage to analyze the impact of the regularization procedure on the predictions of the model. In Fig. 8 we show our results for the  $\rho_{3\perp}$  mass together with those obtained in Ref. [22] and Ref. [57]. To carry out a proper comparison, in our model we have taken  $\alpha = 0.5$  and have set to zero the  $\rho_{0\perp} - \rho_{3\perp}$  mixing contributions,



as done in those works (in which the  $\rho_{0\perp}$  state is not included). Notice that this case corresponds to the solid line in the right panel of Fig. 7. In Ref. [22], divergent integrals are regularized through the introduction of Lorentzian-like form factors, both for vacuum and  $B$ -dependent contributions. On the other hand, in Ref. [57] the regularization is carried out using the MFIR method, as in the present work. However, to deal with vacuum-like terms the authors of Ref. [57] choose a Pauli-Villars regularization, instead of the 3D-cutoff scheme considered here. From Fig. 8 it is seen that our results for  $m_{\rho_{3\perp}}$  (black solid line) are quite similar to those found in Ref. [57] (red dotted line), indicating that they are not too much sensitive to the prescription used for the regularization of vacuum-like terms, once the MFIR method is implemented. Meanwhile, the  $\rho_{3\perp}$  mass obtained by means of a form factor regularization (blue dashed line) shows a much stronger dependence on the magnetic field, specially for large values of  $eB$ . These results are consistent with those found in Ref. [65] for the regularization scheme dependence of the condensates in the presence of the magnetic field.

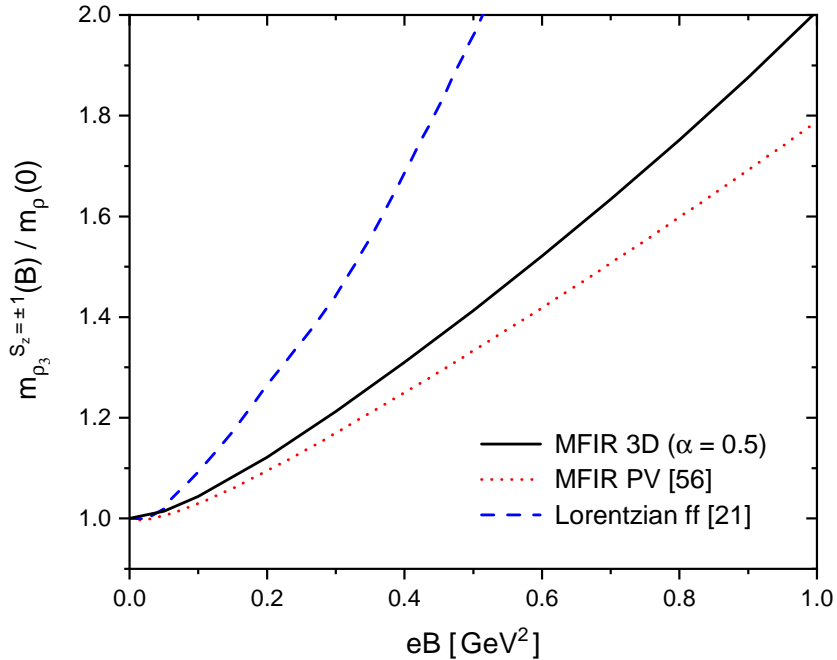


Figure 8. (Color online) Mass of the  $\rho$  meson with  $S_z = \pm 1$  for the case in which  $\alpha = 0.5$  and there is no mixing between pseudoscalar and vector meson states. Results quoted in the literature using other regularization methods are also shown.

Finally, in Fig. 9 we compare our results for the case  $\alpha = 0.1$  (dashed and dotted lines in the central panel of Fig. 7) with those quoted in Ref. [52] for the  $\rho_{u\perp}$  mass using LQCD calculations. In fact, these lattice results are obtained for a large vacuum pion mass of about 400 MeV; the comparison still makes sense, however, since we have checked that our results are rather robust under changes in the current quark masses leading to such a large value of  $m_\pi$ . Considering the large error bars, from the figure one observes that LQCD results seem to indicate an enhancement of  $m_{\rho_{u\perp}}$  when the magnetic field is increased, in agreement with the predictions from the NJL model. This qualitative behavior has been also found in previous LQCD studies [45, 49, 50, 58].

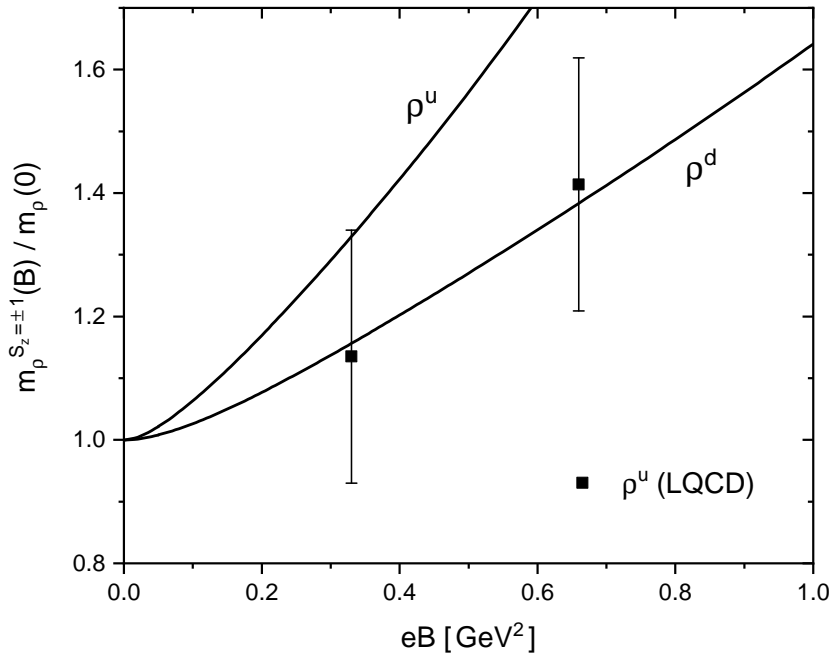


Figure 9. (Color online) Masses of  $S_z = \pm 1$  vector meson states for  $\alpha = 0.1$ , compared with LQCD results given in Ref. [52].

#### D. $B$ -dependent four-fermion couplings

As mentioned in the Introduction, while local NJL-like models are able to reproduce the magnetic catalysis (MC) effect at vanishing temperature, they fail to describe the so-called inverse magnetic catalysis (IMC) observed in lattice QCD. Among the possible ways to deal

with this problem, one of the simplest approaches is to allow the model coupling constants to depend on the magnetic field. With this motivation, we explore in this subsection the possibility of considering a magnetic field dependent coupling  $g(eB)$ . For definiteness, we adopt for this function the form proposed in Ref. [26], namely

$$g(eB) = g \mathcal{F}(eB) , \quad (41)$$

where

$$\mathcal{F}(eB) = \kappa_1 + (1 - \kappa_1) e^{-\kappa_2 (eB)^2} , \quad (42)$$

with  $\kappa_1 = 0.321$ ,  $\kappa_2 = 1.31 \text{ GeV}^{-2}$ . Assuming this form for  $g(eB)$ , the effective quark masses are found to be less affected by the presence of the magnetic field than in the case of a constant  $g$ . In fact, they show a non-monotonous behavior for increasing  $B$ , resembling the results found in Refs. [38, 72]. It should be stressed that in spite of the rather different behavior of the dynamical quark masses, a similar zero-temperature magnetic catalysis effect is obtained both for a constant  $g$  and for a variation with  $B$  of the form given by Eq. (42).

Regarding the vector meson sector, one has to choose some assumption for the  $B$  dependence of the vector coupling constant. One possibility is to suppose that, due to their common gluonic origin, the vector couplings are affected by the magnetic field in the same way as the scalar and pseudoscalar ones. That is to say, one could take  $g_v(eB) = g_v \mathcal{F}_v(eB)$ , with  $\mathcal{F}_v(eB) = \mathcal{F}(eB)$ . Under these assumptions, we have obtained numerical results for the behavior of meson masses with the magnetic field. The curves for the case  $\alpha = 0.1$  are given in Fig. 10, where we also show the  $q\bar{q}$  production thresholds (dotted lines).

By comparison with the results in Fig. 3 and Fig. 6, it can be observed that the  $B$  dependence of the couplings has a significant qualitative effect only in the case of the  $\tilde{\omega}$  state. It is found that the mass of this state follows quite closely the position of the lowest  $q\bar{q}$  production threshold,  $2M_d$ , which —as stated— does get affected by the  $B$  dependence of  $g$ . The behavior of the masses of the other mesons do not change qualitatively with respect to the case  $g = \text{constant}$ , and something similar happens with their composition and their dependence on  $\alpha$ . In particular, the results for the ratio  $r_\pi = m_{\tilde{\pi}}(eB)/m_\pi(0)$  are almost identical to those obtained in Sect. III B (solid line in Fig. 5).

Given the fact that  $g_v(eB)$  is not so well constrained as in the case of the scalar coupling, one can, in principle, introduce a new function  $\mathcal{F}_v(eB)$ , different from  $\mathcal{F}(eB)$ . The freedom in the election of this function can be used to reproduce the results for the ratio  $r_\pi$  obtained

through LQCD calculations. It can be seen, however, that in this case the masses of the  $S_z = \pm 1$  vector mesons increase even faster than in the case in which  $B$ -independent couplings are used.

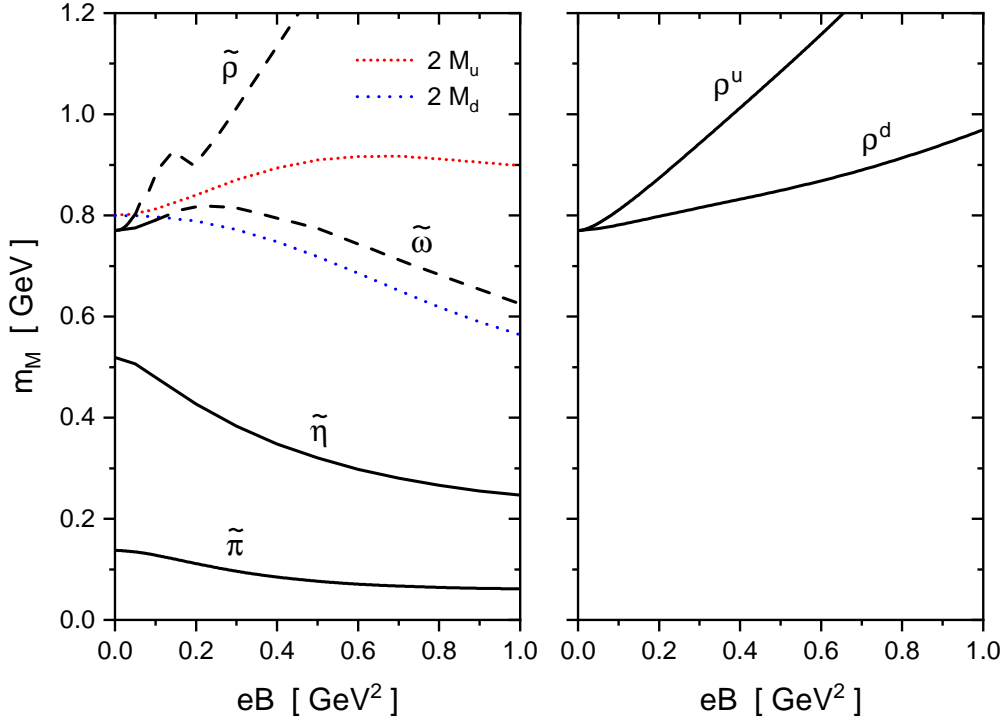


Figure 10. (Color online) Left (right) panel: Masses of the  $S_z = 0$  ( $S_z = \pm 1$ ) meson states as functions of  $eB$ , for  $B$ -dependent couplings  $g(eB)/g = g_v(eB)/g_v = \mathcal{F}(eB)$  [see Eq. (42)]. The results correspond to the case  $\alpha = 0.1$ .

#### IV. CONCLUSIONS

In this work we have studied the mass spectrum of light neutral pseudoscalar and vector mesons in the presence of an external uniform magnetic field  $\vec{B}$ . For this purpose we have considered a two-flavor NJL-like model in the Landau gauge. This model includes isoscalar and isovector couplings in the scalar-pseudoscalar sector and in the vector sector. A flavor mixing term in the scalar-pseudoscalar sector, regulated by a constant  $\alpha$ , has also been included. For  $\alpha = 0$  there is not flavor mixing, but flavor degeneracy gets broken by the

magnetic field and  $M_u \neq M_d$ , while for  $\alpha = 0.5$  one has maximum flavor mixing, as in the case of the standard version of the NJL model, and in this case  $M_u = M_d$ . To account for the usual divergences of the NJL model, we have considered here the magnetic field independent regularization (MFIR) method, which has been shown to reduce the dependence of the results on the model parameters. It should be stressed that for neutral mesons the contributions to the polarization functions arising from Schwinger phases in quark propagators get cancelled; as a consequence, the polarization functions turn out to be diagonal in the usual momentum basis.

It is important to note that the presence of an electromagnetic field allows for isospin mixing. In addition, the axial character of the magnetic field together with the loss of rotational invariance lead to pseudoscalar-vector mixing. These mixing contributions are usually forbidden by isospin and angular momentum conservation. However, they arise and may become important in the presence of the external magnetic field. Although full rotational invariance is broken, invariance under rotations around the magnetic field direction survives. Therefore, the projection of the vector meson spin in the field direction,  $S_z$ , is the observable that organizes the obtained results. Our analysis shows that for the determination of the masses (i.e., if particles are taken at rest), the scalar mesons, which in our case include the  $f_0$  (or  $\sigma$ ) and  $a_0^0$  states, mix with each other but decouple from other mesons. Thus, they can be disregarded in the analysis of the pseudoscalar and vector meson masses. The remaining meson space can be separated into three subspaces: pseudoscalar and vector mesons with  $S_z = 0$ , including  $\pi^0$ ,  $\eta$ ,  $\rho^0$  and  $\omega$ , which mix with each other; vector mesons with  $S_z = +1$ , including  $\rho^0$  and  $\omega$  mesons; same as before, with  $S_z = -1$ .

Regarding the  $S_z = 0$  sector, we observe two different behaviors for the meson masses. The masses of the two lightest mesons, which we have called  $\tilde{\pi}$  and  $\tilde{\eta}$ , are determined by the underlying symmetries and their breaking pattern. In the presence of the magnetic field, with  $\alpha = 0$ , one has a “residual”  $U(1)_{T^3} \otimes U(1)_{T^3,A} \otimes U(1)_A$  chiral symmetry, explicitly broken only by a (small) current mass term,  $m_c \neq 0$ , which guarantees the pseudo-Goldstone character of these two states. We have shown that flavor degeneracy gets broken by the magnetic field and mass eigenstates are separated into particles with pure  $u$  or  $d$  quark content. For  $\alpha = 0.1$ , which leads to a reasonable value for the  $\eta$  mass in the absence of the magnetic field, the  $U(1)_A$  symmetry is broken and only one pseudo-Goldstone boson,  $\tilde{\pi}$ , survives. From our results, we can conclude that even for magnetic field values as large as  $eB = 1 \text{ GeV}^2$ , the  $\tilde{\pi}$

state is mostly a pseudoscalar isovector (third component) and  $\tilde{\eta}$  is mostly a pseudoscalar isoscalar. Increasing the magnetic field intensity from a low value of  $eB = 0.05 \text{ GeV}^2$  to  $eB = 1 \text{ GeV}^2$  we observe that the  $u$  content of the  $\tilde{\pi}$  and the  $d$  content of the  $\tilde{\eta}$  get enhanced.

On the other hand, regarding the quark structure of the two heaviest mesons, which we call  $\tilde{\omega}$  and  $\tilde{\rho}$ , it is found that even for a low value of the magnetic field,  $eB = 0.05 \text{ GeV}^2$ , the mass eigenstates turn out to be clearly dominated by the quark flavor content and spin orientation. This is what we could expect, since the magnetic field tends to separate quarks according to their electric charges, and favors that their magnetic moments be orientated parallel to the field direction.

The lack of confinement in the NJL model implies that the polarization functions get absorptive contributions, related with  $q\bar{q}$  pair production, beyond certain thresholds. In the presence of the magnetic field, the position of each threshold is flavor and spin dependent, in such a way that for  $S_z = 0$  we have thresholds for meson mass values  $m_f = 2 M_f$ , while for  $S_z = \pm 1$  the thresholds rise to higher values  $m_f = M_f + \sqrt{M_f^2 + 2 B_f}$ . As a consequence, we find that  $\tilde{\omega}$  and  $\tilde{\rho}$  states with  $S_z = 0$  enter into the continuum for values of the magnetic field around  $eB \sim 0.1 \text{ GeV}^2$ , whereas  $S_z = \pm 1$  meson masses always lie under  $q\bar{q}$  production thresholds for the considered range of values of  $eB$ . A common result for all these states is that their masses show an appreciable growth when the magnetic field varies from zero to  $eB = 1 \text{ GeV}^2$ . In the case of  $S_z = \pm 1$ , the model reproduces reasonably well present LQCD results for  $\rho_\perp^u$ , taking into account the uncertainties in LQCD simulations.

We have observed that the mass of the lightest state,  $\tilde{\pi}$ , gets reduced as the magnetic field increases. This behavior reproduces the trend of existing LQCD results. However, our results overestimate the mass reduction as compared to the one found in LQCD simulations. It is seen that this reduction is significantly affected by the mixing between pseudoscalar and vector components, a fact that turns out to be independent of the value of the flavor mixing parameter  $\alpha$ . From an analytical perturbative analysis, we have carefully studied how a small value of the vector components in the  $\tilde{\pi}$  state can lead to a significant reduction of its mass. It is seen that both the mixture of the  $\pi$  channel with the  $\omega$  and  $\rho$  channels contribute to this mass shrinkage.

While local NJL-like models are able to reproduce the magnetic catalysis effect at vanishing temperature, they fail to lead to the so-called inverse magnetic catalysis. One of the simplest ways to deal with this problem is to allow that the model coupling constants depend

on the magnetic field. With this motivation, we have explored the possibility of considering magnetic field dependent couplings  $g(eB)$  and  $g_v(eB)$ . For definiteness we take the same dependence on  $B$  for both couplings; in that case, our results show that, for any value of  $\alpha$ , the mass of the  $\tilde{\omega}$  state with  $S_z = 0$  is the only one that becomes significantly modified with respect to the case in which  $g$  and  $g_v$  do not depend on the magnetic field. In particular, the  $B$ -dependence of the ratio  $r_\pi = m_{\tilde{\pi}}(eB)/m_\pi(0)$  is almost identical to that obtained when the couplings  $g$  and  $g_v$  are kept constant. If one allows for different  $B$  dependences for  $g$  and  $g_v$  it is possible to improve on the agreement with LQCD results for this ratio. However, this implies a rather strong enhancement in the masses of  $S_z = \pm 1$  vector meson states, leading to a rather large discrepancy with LQCD results in Ref. [52].

For simplicity, in the present work we have not taken into account the axial vector interactions. The influence of these degrees of freedom in the magnetic field dependence of light neutral meson masses, and, in particular, on the ratio  $r_\pi$ , is certainly an issue that deserves further investigation. It would be also interesting to study the effect of the inclusion of quark anomalous magnetic moments. We expect to report on these issues in future publications.

## ACKNOWLEDGEMENTS

We are grateful to M.F. Izzo Villafa e for helpful discussions at the early stages of this paper. This work has been partially funded by CONICET (Argentina) under Grant No. PIP17-700, by ANPCyT (Argentina) under Grants No. PICT17-03-0571 and PICT19-0792, by the National University of La Plata (Argentina), Project No. X284, by Ministerio de Ciencia e Innovaci n and Agencia Estatal de Investigaci n (Spain) MCIN/AEI/10.13039/501100011033 and European Regional Development Fund Grant PID2019- 105439 GB-C21, by EU Horizon 2020 Grant No. 824093 (STRONG-2020), and by Conselleria de Innovaci n, Universidades, Ciencia y Sociedad Digital, Generalitat Valenciana, GVA PROMETEO/2021/083.

NNS would like to thank the Department of Theoretical Physics of the University of Valencia, where part of this work was carried out, for their hospitality within the visiting professor program of the University of Valencia.

## APPENDIX A: REGULARIZED $B = 0$ POLARIZATION FUNCTIONS

In this appendix we give the expressions for the regularized  $B = 0$  pieces of the polarization functions,  $\hat{J}_{MM'}^{0,\text{reg}}(q)$ , defined within the MFIR scheme. As stated, it can be easily seen that these are zero for  $M \neq M'$ , while for  $M = M'$  one has

$$\begin{aligned}\hat{J}_{\pi^a\pi^a}^{0,\text{reg}}(q) &= -N_c \sum_f \left[ I_{1f} + q^2 I_{2f}(q^2) \right], \\ \hat{J}_{\rho_\mu^a \rho_\nu^a}^{0,\text{reg}}(q) &= \frac{2N_c}{3} \sum_f \left[ (2M_f^2 - q^2) I_{2f}(q^2) - 2M_f^2 I_{2f}(0) \right] \left( \delta_{\mu\nu} - \frac{q_\mu q_\nu}{q^2} \right).\end{aligned}\quad (\text{A1})$$

Here, the integrals  $I_{1f}$  and  $I_{2f}(q^2)$  are defined as

$$I_{1f} = 4 \int_p \frac{1}{M_f^2 + p^2}, \quad I_{2f}(q^2) = -2 \int_p \frac{1}{(M_f^2 + p_+^2)(M_f^2 + p_-^2)}, \quad (\text{A2})$$

with  $p^\pm = p \pm q/2$ . Within the 3D-cutoff regularization scheme used in this work, the first of these integrals is given by

$$I_{1f} = \frac{1}{2\pi^2} \left[ \Lambda^2 r_{\Lambda f} + M_f^2 \ln \left( \frac{M_f}{\Lambda (1 + r_{\Lambda f})} \right) \right], \quad (\text{A3})$$

where we have defined  $r_{\Lambda f} \equiv \sqrt{1 + M_f^2/\Lambda^2}$ . In the case of  $I_{2f}(q^2)$ , we note that in order to determine the meson masses, the external momentum  $q$  has to be extended to the region  $q^2 < 0$ . Hence, we find it convenient to write  $q^2 = -m^2$ , where  $m$  is a positive real number. Then, within the 3D-cutoff regularization scheme, the regularized real part of  $I_{2f}(-m^2)$  can be written as

$$\text{Re} [I_{2f}(-m^2)] = -\frac{1}{4\pi^2} \left[ \text{arcsinh} \left( \frac{\Lambda}{M_f} \right) - F_f \right], \quad (\text{A4})$$

where

$$F_f = \begin{cases} \sqrt{4M_f^2/m^2 - 1} \arctan \left( \frac{1}{r_{\Lambda f} \sqrt{4M_f^2/m^2 - 1}} \right) & \text{if } m^2 < 4M_f^2 \\ \sqrt{1 - 4M_f^2/m^2} \text{arccoth} \left( \frac{1}{r_{\Lambda f} \sqrt{1 - 4M_f^2/m^2}} \right) & \text{if } 4M_f^2 < m^2 < 4(M_f^2 + \Lambda^2) \\ \sqrt{1 - 4M_f^2/m^2} \text{arctanh} \left( \frac{1}{r_{\Lambda f} \sqrt{1 - 4M_f^2/m^2}} \right) & \text{if } m^2 > 4(M_f^2 + \Lambda^2) \end{cases}.$$

For the regularized imaginary part we get

$$\text{Im} [I_{2f}(-m^2)] = \begin{cases} -\frac{1}{8\pi} \sqrt{1 - 4M_f^2/m^2} & \text{if } 4M_f^2 < m^2 < 4(M_f^2 + \Lambda^2) \\ 0 & \text{otherwise} \end{cases}. \quad (\text{A5})$$



## APPENDIX B: INTEGRALS $I_{nf}^{\text{mag}}(-m^2)$ FOR $m > 2M_f$

The expressions for the integrals  $I_{nf}^{\text{mag}}(-m^2)$  for  $n = 2, \dots, 5$  given in Eqs. (30) are only valid when  $m < 2M_f$ . For  $m > 2M_f$ , it happens that the corresponding integrands can become divergent at some points within the integration domain, leading to divergent integrals. However, we can get finite results by considering the analytical extension of the functions in Eqs. (30). For this purpose it is worth taking into account that the Feynman quark propagators originally contain “ $i\epsilon$ ” terms, which can be easily recovered in the integrands of Eqs. (30) through the replacement  $M_f^2 \rightarrow M_f^2 - i\epsilon$  (note that this implies the replacement  $\bar{x}_f \rightarrow \bar{x}_f - i\epsilon$ ). Once this is done, one can proceed by using the digamma recurrence relation

$$\psi(x) = \psi(x + n + 1) - \sum_{j=0}^n \frac{1}{x + j} , \quad (\text{B1})$$

and taking  $\epsilon \rightarrow 0^+$  through a generalized version of the Sokhotski-Plemelj formula [see e.g. Eq. (A8) of Ref. [38]]. In this way, we find that for  $m > 2M_f$  the integrals  $I_{nf}^{\text{mag}}(-m^2)$ ,  $n = 2, \dots, 5$ , can be extended to

$$\begin{aligned} I_{2f}^{\text{mag}}(-m^2) = & \frac{1}{8\pi^2} \left[ \int_0^1 dv \, \psi(\bar{x}_f + N + 1) \right. \\ & \left. - \ln x_f + 2 - 2\beta_0 \operatorname{arctanh} \beta_0 + \frac{4B_f}{m^2} \sum_{n=0}^N \frac{\alpha_n}{\beta_n} \operatorname{arctanh} \beta_n \right] \\ & + \frac{i}{8\pi} \left[ \beta_0 - \frac{2B_f}{m^2} \sum_{n=0}^N \frac{\alpha_n}{\beta_n} \right] , \end{aligned} \quad (\text{B2})$$

$$I_{3f}^{\text{mag}}(-m^2) = -\frac{Q_f M_f}{\pi^2 m} \left[ \frac{\operatorname{arctanh} \beta_0}{\beta_0} - i \frac{\pi}{2\beta_0} \right] , \quad (\text{B3})$$

$$\begin{aligned} I_{4f}^{\text{mag}}(-m^2) = & -I_{1f}^{\text{mag}} + T_f^+(-m^2) + T_f^-(-m^2) \\ & - \frac{m^2}{16\pi^2} \left[ 4\beta_0 \left(1 - \frac{1}{3}\beta_0^2\right) \operatorname{arctanh} \beta_0 + \left(\frac{7}{3} - \beta_0^2\right) \ln x_f + \frac{4}{3}\beta_0^2 - \frac{38}{9} \right] \\ & + \frac{i m^2}{8\pi} \left[ \beta_0 \left(1 - \frac{1}{3}\beta_0^2\right) - \theta(m - m_f^-) \frac{4B_f}{m^2} \sum_{n=0}^{N^-} \frac{(2\lambda - 2n - 1)}{r_n} \right] , \end{aligned} \quad (\text{B4})$$

$$\begin{aligned}
I_{5f}^{\text{mag}}(-m^2) = & \frac{1}{8\pi^2} \left[ \int_0^1 dv (1-v^2) \psi(\bar{x}_f + N + 1) \right. \\
& - \frac{2}{3} \left( \ln x_f - \frac{8}{3} + \beta_0^2 + \beta_0(3 - \beta_0^2) \operatorname{arctanh} \beta_0 \right) \\
& + \frac{4B_f}{m^2} \sum_{n=0}^N \frac{\alpha_n}{\beta_n} [\beta_n + (1 - \beta_n^2) \operatorname{arctanh} \beta_n] \Big] \\
& + \frac{i}{8\pi} \left[ \beta_0(1 - \frac{1}{3}\beta_0^2) - \frac{2B_f}{m^2} \sum_{n=0}^N \frac{\alpha_n}{\beta_n} (1 - \beta_n^2) \right]. \tag{B5}
\end{aligned}$$

Here, we have used the definition  $\alpha_n = 2 - \delta_{0n}$ , together with

$$\beta_n = \sqrt{1 - \frac{4(M_f^2 + 2nB_f)}{m^2}}, \quad r_n = \sqrt{1 - 4\lambda(2n+1) + 4\lambda^2\beta_0^2}, \quad N = \text{Floor} [\lambda\beta_0^2/2],$$

where  $\lambda = m^2/(4B_f)$ . In the expression of  $I_{4f}^{\text{mag}}(-m^2)$  the integral  $I_{1f}^{\text{mag}}$  is that given by Eq. (15), and we have introduced the functions  $T_f^\pm(-m^2)$  given by

$$\begin{aligned}
T_f^\pm(-m^2) = & \frac{m^2}{32\pi^2} \int_0^1 dv (v^2 \pm v/\lambda + \gamma) \psi(\bar{x}_f + (1 \pm v)/2 + \theta(m - m_f^\pm)(1 + N^\pm)) \\
& - \frac{B_f}{4\pi^2} \theta(m - m_f^\pm) \sum_{n=0}^{N^\pm} \left\{ 1 - \frac{(2\lambda - 2n - 1)}{r_n} \ln \left[ \frac{(2\lambda - r_n \pm 1)|r_n \pm 1|}{(2\lambda + r_n \pm 1)(r_n \mp 1)} \right] \right\}, \tag{B6}
\end{aligned}$$

with  $\gamma = 2 - \beta_0^2 = 1 + 4M_f^2/m^2$ , and

$$m_f^- = M_f + \sqrt{M_f^2 + 2B_f}, \quad m_f^+ = 2\sqrt{M_f^2 + B_f}. \tag{B7}$$

The integers  $N^\pm$  have been defined as

$$N^- = \text{Floor} [r_0^2/(8\lambda)], \quad N^+ = \text{Floor} [(\lambda\beta_0^2 - 1)/2]. \tag{B8}$$

### APPENDIX C: A SIMPLIFIED MODEL FOR THE LOWEST STATE OF THE $S_z = 0$ SECTOR

In this appendix we present a simplified model to analyze the mass and composition of the lowest state of the  $S_z = 0$  meson sector. As seen in Sec. III B (see the discussion concerning Fig. 4), the mass of this state, while almost independent of the value of  $\alpha$ , is significantly affected by the existence of a mixing between pseudoscalar and vector meson states. Thus, to simplify the analysis we consider the case  $\alpha = 0.5$ , in which the relevant basis is only composed by the states  $\pi_3$ ,  $\rho_{3\parallel}$  and  $\rho_{0\parallel}$ . In addition, one has  $M_u = M_d \equiv M$

for any value of  $eB$ . Assuming as in the main text  $g_{v_0} = g_{v_3} = g_v$ , it is easy to see that the ratio between the off-diagonal  $\pi_3\rho_{3\parallel}$  and  $\pi_3\rho_{0\parallel}$  mixing matrix elements is given by  $G_{\parallel\pi_3\rho_3}/G_{\parallel\pi_3\rho_0} = (B_u - B_d)/(B_u + B_d) = 1/3$ . Hence, to simplify the problem even further, in what follows we only consider the  $\pi_3 - \rho_{0\parallel}$  system (see, however, discussion at the end of this appendix). To check whether we are capturing the main effect of pseudoscalar-vector meson mixing on the  $\tilde{\pi}$  mass it is useful to consider the ratio  $r_\pi = m_{\tilde{\pi}}(eB)/m_\pi(0)$ . Assuming that  $g$  and  $g_v$  do not depend on the magnetic field, and taking  $\alpha = 0.1$ , for  $eB = 1 \text{ GeV}^2$  we get  $r_\pi = 0.32$  for the full  $\pi_0 - \pi_3 - \rho_{0\parallel} - \rho_{3\parallel}$  system, to be compared with the values  $r_\pi = 0.38$ , obtained when we consider only the  $\pi_3 - \rho_{0\parallel}$  system, and  $r_\pi = 0.92$ , obtained for the case in which there is no mixing at all. These values clearly support our approximation of the full system by the much simpler  $\pi_3\rho_{0\parallel}$  one. It should be stressed that even in this simplified situation the lowest mass state is still found to be strongly dominated by the  $\pi_3$  contribution. In fact, for  $eB = 1 \text{ GeV}^2$  we get  $c_{\rho_{0\parallel}}^{(1)} = -0.083$ , close to the value  $-0.0797$  obtained for the full system (see Table I). Defining a mixing angle  $\theta$  by  $\tan \theta = c_{\rho_{0\parallel}}^{(1)}/c_{\pi_3}^{(1)}$ , this implies  $\theta \simeq -5^\circ$ .

The strong dominance of the  $\pi_3$  contribution to the  $\tilde{\pi}$  state suggests that one should be able to determine the mixing effect on  $m_{\tilde{\pi}}$  using first order perturbation theory. On the other hand, this appears to be in contradiction with the aforementioned significant reduction of the  $\tilde{\pi}$  mass. To get a better understanding of the situation, it is convenient to carry out some further approximations. The relevant mixing matrix elements to be considered are

$$\begin{aligned} G_{\parallel\pi_3\pi_3} &= \frac{1}{2g} - N_c \sum_f [(I_{1f} + I_{1f}^{\text{mag}}) - m^2(I_{2f}(-m^2) + I_{2f}^{\text{mag}}(-m^2))] , \\ G_{\parallel\pi_3\rho_0} &= \frac{i N_c s_B B_e \arctan \left( 1/\sqrt{4M^2/m^2 - 1} \right)}{2\pi^2 \sqrt{1 - m^2/4M^2}} , \\ G_{\parallel\rho_0\rho_0} &= \frac{1}{2g_v} + N_c \sum_f \left[ \frac{2}{3} \left[ (2M^2 + m^2)I_{2f}(-m^2) - 2M^2 I_{2f}(0) \right] + m^2 I_{5f}^{\text{mag}}(-m^2) \right] , \end{aligned} \quad (\text{C1})$$

where we have denoted  $B_e = |eB|$  and  $s_B = \text{sign}(B)$ . For the  $\tilde{\pi}$  state, we have  $m^2/(4M^2) \ll 1$  (for our parametrization we find  $m^2/(4M^2) \approx 0.03$  at vanishing magnetic field, and even a smaller value at  $eB = 1 \text{ GeV}^2$ ). Thus, we can obtain a good approximation to these matrix elements by expanding up to  $\mathcal{O}(m^2/4M^2)$ . In this way we get a mixing matrix of the form

$$G_{\parallel}^{(\pi_3\rho_0)} = \begin{pmatrix} a - b m^2 & i c m \\ -i c m & d - b' m^2 \end{pmatrix} , \quad (\text{C2})$$

where

$$a = \frac{m_c}{2gM} , \quad c = \frac{N_c s_B B_e}{4\pi^2 M} , \quad d = \frac{1}{2g_v} , \quad b' = \frac{2b}{3} + \frac{N_c}{18\pi^2} \frac{\Lambda^3}{(\Lambda^2 + M^2)^{3/2}} \quad (\text{C3})$$

and

$$b = \frac{N_c}{8\pi^2} \left[ 4 \operatorname{arcsinh} \frac{\Lambda}{M} - \frac{4\Lambda}{\sqrt{\Lambda^2 + M^2}} - \frac{B_e}{M^2} + \ln \frac{9M^4}{8B_e^2} - \psi \left( \frac{3M^2}{4B_e} \right) - \psi \left( \frac{3M^2}{2B_e} \right) \right] . \quad (\text{C4})$$

We note that here the gap equation has been used to get the expression for  $a$ . Given the model parameters, these coefficients can be easily computed for a given value of  $B_e$ .

Keeping terms up to the leading order in  $m^2$ , one gets in this way

$$m_{\tilde{\pi}}^2 = \frac{a d}{a b' + b d + c^2} . \quad (\text{C5})$$

In addition, it can be seen that  $a/d = (g_{v0}/g)(m_c/M) \ll 1$ , and consequently  $ab' \ll bd$ .

Using this approximation we obtain

$$m_{\tilde{\pi}} = \frac{\bar{m}_{\tilde{\pi}}}{\sqrt{1 + c^2/(b d)}} , \quad (\text{C6})$$

where  $\bar{m}_{\tilde{\pi}} = \sqrt{a/b}$  is the mass of the lightest state if there is no mixing at all. Within the same approximation, the coefficient of the  $\rho_{0\parallel}$  piece of the lightest state is given by

$$c_{\rho_{0\parallel}}^{(1)} = -\frac{m_{\tilde{\pi}} c}{d} . \quad (\text{C7})$$

The numerical values for the above quantities can be calculated from Eqs. (C3), (C4). For a large magnetic field  $eB = 1 \text{ GeV}^2$ , assuming that the coupling constants are independent of  $B$ , we get  $r_{\pi} = 0.39$  and  $c_{\rho_{0\parallel}}^{(1)} = -0.084$ , in excellent agreement with the results quoted above for the  $\pi_3 \rho_{0\parallel}$  system. This confirms the validity of the approximations made so far.

It is also interesting to note that the expression for  $m_{\tilde{\pi}}$  given in Eq. (C6) implies

$$b(m_{\tilde{\pi}}^2 - \bar{m}_{\tilde{\pi}}^2) = -\frac{m_{\tilde{\pi}}^2 c^2}{d} . \quad (\text{C8})$$

This expression, together with the one for  $c_{\rho_{0\parallel}}^{(1)}$  in Eq. (C7), are the relations that one would obtain from a first-order perturbation analysis of the system described by the matrix in Eq. (C2) when  $d \gg a + (b' - b)m^2$ , a condition that is always well satisfied in our case. One can observe that the somewhat unexpectedly “large” value of the mass shift arises from the small value of the coefficient  $b$ , which is found to be about 0.034 for  $eB = 1 \text{ GeV}^2$  (assuming  $B$ -independent couplings). In a conventional eigenvalue problem, one would have  $b = 1$ .

Finally, we note that the effect on this game of the  $\rho_{3\parallel}$  meson, so far neglected, can be easily taken into account at this stage. Since, as shown above, the  $G_{\parallel\pi_3\rho_0}$  matrix element can be treated perturbatively, and  $G_{\parallel\pi_3\rho_3}$  is even 3 times smaller, one can account for the  $\rho_{3\parallel}$  meson just replacing the factor  $c^2$  in Eq. (C6) by  $10/9 c^2$ . The resulting expression for  $m_{\tilde{\pi}}$  can be rewritten as

$$m_{\tilde{\pi}} = \frac{\bar{m}_{\tilde{\pi}}}{\sqrt{1 + \kappa \bar{m}_{\tilde{\pi}}^2 B_e^2 / M}} \quad , \quad (\text{C9})$$

where  $\kappa = 5N_c^2 g g_v / (18\pi^4 m_c)$ . To obtain this expression we have made use of Eq. (C3) together with the relation  $b = a / \bar{m}_{\tilde{\pi}}^2 = m_c / (2gM\bar{m}_{\tilde{\pi}}^2)$ .

It should be emphasized that although the numerical values quoted in this appendix correspond to the case in which the couplings  $g$  and  $g_v$  are kept fixed, Eq. (C9) can be shown to be approximatively valid also when they depend on  $B$  as considered in Sec. III D.

- 
- [1] D. E. Kharzeev, K. Landsteiner, A. Schmitt and H. U. Yee, Lect. Notes Phys. **871**, 1-11 (2013) [arXiv:1211.6245 [hep-ph]].
  - [2] J. O. Andersen, W. R. Naylor and A. Tranberg, Rev. Mod. Phys. **88**, 025001 (2016) [arXiv:1411.7176 [hep-ph]].
  - [3] V. A. Miransky and I. A. Shovkovy, Phys. Rept. **576**, 1-209 (2015) [arXiv:1503.00732 [hep-ph]].
  - [4] T. Vachaspati, Phys. Lett. B **265**, 258-261 (1991)
  - [5] D. Grasso and H. R. Rubinstein, Phys. Rept. **348**, 163-266 (2001) [arXiv:astro-ph/0009061 [astro-ph]].
  - [6] R. C. Duncan and C. Thompson, Astrophys. J. Lett. **392**, L9 (1992).
  - [7] C. Kouveliotou *et al.*, Nature **393**, 235-237 (1998).
  - [8] V. Skokov, A. Y. Illarionov and V. Toneev, Int. J. Mod. Phys. A **24**, 5925-5932 (2009) [arXiv:0907.1396 [nucl-th]].
  - [9] V. Voronyuk, V. D. Toneev, W. Cassing, E. L. Bratkovskaya, V. P. Konchakovski and S. A. Voloshin, Phys. Rev. C **83**, 054911 (2011) [arXiv:1103.4239 [nucl-th]].
  - [10] D. E. Kharzeev, L. D. McLerran and H. J. Warringa, Nucl. Phys. A **803**, 227-253 (2008) [arXiv:0711.0950 [hep-ph]].
  - [11] K. Fukushima, D. E. Kharzeev and H. J. Warringa, Phys. Rev. D **78**, 074033 (2008) [arXiv:0808.3382 [hep-ph]].

- [12] D. E. Kharzeev, J. Liao, S. A. Voloshin and G. Wang, Prog. Part. Nucl. Phys. **88**, 1-28 (2016) [arXiv:1511.04050 [hep-ph]].
- [13] S. P. Klevansky and R. H. Lemmer, Phys. Rev. D **39**, 3478-3489 (1989)
- [14] V. P. Gusynin, V. A. Miransky and I. A. Shovkovy, Nucl. Phys. B **462**, 249-290 (1996) [arXiv:hep-ph/9509320 [hep-ph]].
- [15] G. S. Bali, F. Bruckmann, G. Endrodi, Z. Fodor, S. D. Katz, S. Krieg, A. Schafer and K. K. Szabo, JHEP **02**, 044 (2012) [arXiv:1111.4956 [hep-lat]].
- [16] G. S. Bali, F. Bruckmann, G. Endrodi, Z. Fodor, S. D. Katz and A. Schafer, Phys. Rev. D **86**, 071502 (2012) [arXiv:1206.4205 [hep-lat]].
- [17] M. N. Chernodub, Phys. Rev. D **82**, 085011 (2010) [arXiv:1008.1055 [hep-ph]].
- [18] M. N. Chernodub, Phys. Rev. Lett. **106**, 142003 (2011) [arXiv:1101.0117 [hep-ph]].
- [19] V. V. Braguta, P. V. Buividovich, M. N. Chernodub, A. Y. Kotov and M. I. Polikarpov, Phys. Lett. B **718**, 667-671 (2012) [arXiv:1104.3767 [hep-lat]].
- [20] Y. Hidaka and A. Yamamoto, Phys. Rev. D **87**, no.9, 094502 (2013) [arXiv:1209.0007 [hep-ph]].
- [21] C. Li and Q. Wang, Phys. Lett. B **721**, 141-145 (2013) [arXiv:1301.7009 [hep-th]].
- [22] H. Liu, L. Yu and M. Huang, Phys. Rev. D **91**, no.1, 014017 (2015) [arXiv:1408.1318 [hep-ph]].
- [23] S. Fayazbakhsh, S. Sadeghian and N. Sadooghi, Phys. Rev. D **86**, 085042 (2012) [arXiv:1206.6051 [hep-ph]].
- [24] S. Fayazbakhsh and N. Sadooghi, Phys. Rev. D **88**, no.6, 065030 (2013) [arXiv:1306.2098 [hep-ph]].
- [25] S. S. Avancini, W. R. Tavares and M. B. Pinto, Phys. Rev. D **93**, no.1, 014010 (2016) [arXiv:1511.06261 [hep-ph]].
- [26] S. S. Avancini, R. L. S. Farias, M. Benghi Pinto, W. R. Tavares and V. S. Timóteo, Phys. Lett. B **767**, 247-252 (2017) [arXiv:1606.05754 [hep-ph]].
- [27] S. Mao and Y. Wang, Phys. Rev. D **96**, no.3, 034004 (2017) [arXiv:1702.04868 [hep-ph]].
- [28] R. Zhang, W. j. Fu and Y. x. Liu, Eur. Phys. J. C **76**, no.6, 307 (2016) [arXiv:1604.08888 [hep-ph]].
- [29] D. Gómez Dumm, M. F. Izzo Villafañe and N. N. Scoccola, Phys. Rev. D **97**, no.3, 034025 (2018) [arXiv:1710.08950 [hep-ph]].
- [30] Z. Wang and P. Zhuang, Phys. Rev. D **97**, no.3, 034026 (2018) [arXiv:1712.00554 [hep-ph]].

- [31] H. Liu, X. Wang, L. Yu and M. Huang, Phys. Rev. D **97**, 076008 (2018) [arXiv:1801.02174 [hep-ph]].
- [32] M. Coppola, D. Gómez Dumm and N. N. Scoccola, Phys. Lett. B **782**, 155-161 (2018) [arXiv:1802.08041 [hep-ph]].
- [33] S. Mao, Phys. Rev. D **99**, no.5, 056005 (2019) [arXiv:1808.10242 [nucl-th]].
- [34] S. S. Avancini, R. L. S. Farias and W. R. Tavares, Phys. Rev. D **99**, no.5, 056009 (2019) [arXiv:1812.00945 [hep-ph]].
- [35] M. Coppola, D. Gomez Dumm, S. Noguera and N. N. Scoccola, Phys. Rev. D **100**, no.5, 054014 (2019) [arXiv:1907.05840 [hep-ph]].
- [36] G. Cao, Phys. Rev. D **100**, no.7, 074024 (2019) [arXiv:1906.01398 [nucl-th]].
- [37] B. k. Sheng, X. Wang and L. Yu, Phys. Rev. D **105**, no.3, 034003 (2022) [arXiv:2110.12811 [hep-ph]].
- [38] S. S. Avancini, M. Coppola, N. N. Scoccola and J. C. Sodr , Phys. Rev. D **104**, no.9, 094040 (2021) [arXiv:2109.01911 [hep-ph]].
- [39] A. Ayala, R. L. S. Farias, S. Hern ndez-Ortiz, L. A. Hern ndez, D. M. Paret and R. Zamora, Phys. Rev. D **98**, no.11, 114008 (2018) [arXiv:1809.08312 [hep-ph]].
- [40] K. Kamikado and T. Kanazawa, JHEP **03**, 009 (2014) [arXiv:1312.3124 [hep-ph]].
- [41] N. O. Agasian and I. A. Shushpanov, JHEP **10**, 006 (2001) [arXiv:hep-ph/0107128 [hep-ph]].
- [42] J. O. Andersen, JHEP **10**, 005 (2012) [arXiv:1205.6978 [hep-ph]].
- [43] G. Colucci, E. S. Fraga and A. Sedrakian, Phys. Lett. B **728**, 19-24 (2014) [arXiv:1310.3742 [nucl-th]].
- [44] V. D. Orlovsky and Y. A. Simonov, JHEP **09**, 136 (2013) [arXiv:1306.2232 [hep-ph]].
- [45] M. A. Andreichikov, B. O. Kerbikov, E. V. Lushevskaya, Y. A. Simonov and O. E. Solovjeva, JHEP **05**, 007 (2017) [arXiv:1610.06887 [hep-ph]].
- [46] Y. A. Simonov, Phys. Atom. Nucl. **79**, no.3, 455-460 (2016) [arXiv:1503.06616 [hep-ph]].
- [47] M. A. Andreichikov and Y. A. Simonov, Eur. Phys. J. C **78**, 902 (2018) [arXiv:1805.11896 [hep-ph]].
- [48] C. A. Dominguez, M. Loewe and C. Villavicencio, Phys. Rev. D **98**, no.3, 034015 (2018) [arXiv:1806.10088 [hep-ph]].
- [49] E. V. Lushevskaya, O. E. Solovjeva, O. A. Kochetkov and O. V. Teryaev, Nucl. Phys. B **898**, 627-643 (2015) [arXiv:1411.4284 [hep-lat]].

- [50] E. V. Luschevskaya, O. A. Kochetkov, O. V. Teryaev and O. E. Solovjeva, JETP Lett. **101**, no.10, 674-678 (2015)
- [51] B. B. Brandt, G. Bali, G. Endrödi and B. Glässle, PoS **LATTICE2015**, 265 (2016) [arXiv:1510.03899 [hep-lat]].
- [52] G. S. Bali, B. B. Brandt, G. Endrödi and B. Gläße, Phys. Rev. D **97**, no.3, 034505 (2018) [arXiv:1707.05600 [hep-lat]].
- [53] H. T. Ding, S. T. Li, A. Tomiya, X. D. Wang and Y. Zhang, Phys. Rev. D **104**, no.1, 014505 (2021) [arXiv:2008.00493 [hep-lat]].
- [54] M. Kawaguchi and S. Matsuzaki, Phys. Rev. D **93**, no.12, 125027 (2016) [arXiv:1511.06990 [hep-ph]].
- [55] S. Ghosh, A. Mukherjee, M. Mandal, S. Sarkar and P. Roy, Phys. Rev. D **94**, no.9, 094043 (2016) [arXiv:1612.02966 [nucl-th]].
- [56] S. Ghosh, A. Mukherjee, N. Chaudhuri, P. Roy and S. Sarkar, Phys. Rev. D **101**, no.5, 056023 (2020) [arXiv:2003.02024 [hep-ph]].
- [57] S. S. Avancini, R. L. S. Farias, W. R. Tavares and V. S. Timóteo, [arXiv:2202.03328 [hep-ph]].
- [58] E. V. Luschevskaya and O. V. Larina, Nucl. Phys. B **884**, 1-16 (2014) [arXiv:1203.5699 [hep-lat]].
- [59] E. V. Luschevskaya, O. E. Solovjeva and O. V. Teryaev, JHEP **09**, 142 (2017) [arXiv:1608.03472 [hep-lat]].
- [60] U. Vogl and W. Weise, Prog. Part. Nucl. Phys. **27**, 195-272 (1991)
- [61] S. P. Klevansky, Rev. Mod. Phys. **64**, 649-708 (1992)
- [62] T. Hatsuda and T. Kunihiro, Phys. Rept. **247**, 221-367 (1994) [arXiv:hep-ph/9401310 [hep-ph]].
- [63] J. S. Schwinger, Phys. Rev. **82**, 664-679 (1951)
- [64] P. G. Allen, A. G. Grunfeld and N. N. Scoccola, Phys. Rev. D **92**, no.7, 074041 (2015) [arXiv:1508.04724 [hep-ph]].
- [65] S. S. Avancini, R. L. S. Farias, N. N. Scoccola and W. R. Tavares, Phys. Rev. D **99**, no.11, 116002 (2019) [arXiv:1904.02730 [hep-ph]].
- [66] D. P. Menezes, M. Benghi Pinto, S. S. Avancini, A. Perez Martinez and C. Providencia, Phys. Rev. C **79**, 035807 (2009) [arXiv:0811.3361 [nucl-th]].
- [67] G. 't Hooft, Phys. Rept. **142**, 357-387 (1986)



- [68] V. A. Miransky and I. A. Shovkovy, Phys. Rev. D **66**, 045006 (2002) [arXiv:hep-ph/0205348 [hep-ph]].
- [69] A. Ayala, M. Loewe, A. J. Mizher and R. Zamora, Phys. Rev. D **90**, no.3, 036001 (2014) [arXiv:1406.3885 [hep-ph]].
- [70] R. L. S. Farias, K. P. Gomes, G. I. Krein and M. B. Pinto, Phys. Rev. C **90**, no.2, 025203 (2014) [arXiv:1404.3931 [hep-ph]].
- [71] M. Ferreira, P. Costa, O. Lourenço, T. Frederico and C. Providência, Phys. Rev. D **89**, no.11, 116011 (2014) [arXiv:1404.5577 [hep-ph]].
- [72] G. Endrődi and G. Markó, JHEP **08**, 036 (2019) [arXiv:1905.02103 [hep-lat]].
- [73] T. Kunihiro, Phys. Lett. B **219**, 363-368 (1989) [erratum: Phys. Lett. B **245**, 687 (1990)]
- [74] M. Frank, M. Buballa and M. Oertel, Phys. Lett. B **562**, 221-226 (2003) [arXiv:hep-ph/0303109 [hep-ph]].
- [75] V. Bernard, A. H. Blin, B. Hiller, Y. P. Ivanov, A. A. Osipov and U. G. Meissner, Phys. Lett. B **409**, 483-490 (1997) [arXiv:hep-ph/9705438 [hep-ph]].
- [76] S. Borsanyi, G. Endrodi, Z. Fodor, A. Jakovac, S. D. Katz, S. Krieg, C. Ratti and K. K. Szabo, JHEP **11**, 077 (2010) [arXiv:1007.2580 [hep-lat]].